AN EXAMINATION OF THE HANSON CONTRAIL FORECAST ALGORITHM UNDER LOW RELATIVE HUMIDITY CONDITIONS

THESIS

Robert P. Asbury III, Captain, USAF

AFIT/GM/ENP/97M-01

DEPARTMENT OF THE AIR FORCE

AIR UNIVERSITY

AIR FORCE INSTITUTE OF TECHNOLOGY

Wright-Patterson Air Force Base, Ohio

DTIC QUALITY INSPECTED 1

AN EXAMINATION OF THE HANSON CONTRAIL
FORECAST ALGORITHM UNDER LOW
RELATIVE HUMIDITY CONDITIONS

THESIS

Robert P. Asbury III, Captain, USAF

AFIT/GM/ENP/97M-01

19970402 087

AFIT/GM/ENP/97M-01

AN EXAMINATION OF THE HANSON CONTRAIL FORECAST
ALGORITHM UNDER LOW RELATIVE HUMIDITY CONDITIONS

THESIS

Presented to the Faculty of the Graduate School of Engineering

of the Air Force Institute of Technology

Air University

Air Education and Training Command

In Partial Fulfillment of the Requirements for the

Degree of Master of Science in Meteorology

Robert P. Asbury III
Captain, USAF

March 1997

AN EXAMINATION OF THE HANSON CONTRAIL FORECAST ALGORITHM UNDER LOW RELATIVE HUMIDITY CONDITIONS

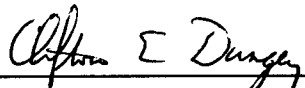Robert P. Asbury III, B.S.
Captain, USAF

Approved:

Lt Col Michael K. Walters
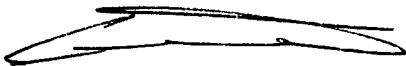Chairman, Advisory Committee

10 MAR 97
Date

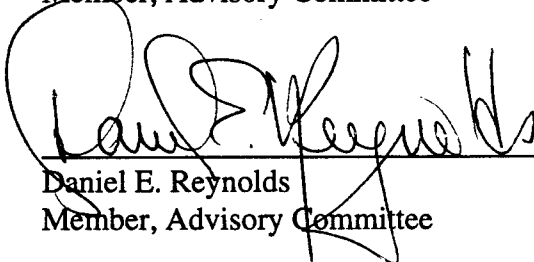Maj Clifton E. Dungey
Member, Advisory Committee

10 MAR 97
Date

Maj Glen P. Perram
Member, Advisory Committee

10 MAR 97
Date

Daniel E. Reynolds
Member, Advisory Committee

10 March 97
Date

Table of Contents

List of Figures

List of Tables

Abstract

Accurate forecasts of contrail occurrence are essential to military aircrews. Although classical forecast methods have been reasonably successful predicting contrails, there is need for improvement at low ambient relative humidity. This thesis examines the performance of the Hanson method, which was developed to provide better contrail forecasts under drier atmospheric conditions. As a secondary objective, the forecast methods of Schumann and Hanson are compared to the algorithm currently in use by the Air Force Global Weather Central (AFGWC).

Data used to validate the forecast methods were collected at Wright-Patterson AFB, using upper-air soundings and observations of commercial aircraft, and at Edwards AFB by the Northrop Corporation. Theoretical contrail forecasts were made for each observation, using the flight level pressure, ambient temperature, and relative humidity. Comparisons were then made between the forecast and actual observation of contrail conditions. Forecast and occurrence data were then statistically analyzed to gauge each method's performance.

All methods detected roughly 75 percent of observed contrails under moist atmospheric conditions. However, the Hanson method's performance dropped sharply when drier atmospheric observations were tested. Schumann's method performed as well

as the AFGWC algorithm under all atmospheric conditions. Based on this research, the

Hanson method is not recommended for operational use.

AN EXAMINATION OF THE HANSON CONTRAIL FORECAST ALGORITHM UNDER LOW RELATIVE HUMIDITY CONDITIONS

1. Introduction

1.1 Background

Condensation trails (contrails) are long cylindrically-shaped clouds, composed of water droplets or ice crystals, which form behind an aircraft when its wake becomes supersaturated with respect to water (AWS/TR-81/001, 1981:1). Contrails may be produced by aerodynamic forces, at relatively high ambient temperatures, or from the mixing of exhaust gases with ambient air, which requires very low temperatures.

Aerodynamic contrails form from adiabatic cooling (by the reduction in air pressure from high-speed flow over an airfoil) and subsequent supersaturation of the trailing vortex system. This phenomenon produces short, transitory contrails which generally develop in areas of maximum pressure decrease, such as the tips of wings or propellers (AWS/TR-81/001, 1981:1). Such contrails form in warm, humid environments and are frequently seen in footage of combat aircraft during the Vietnam War. Since these contrails are short-lived, and usually form during evasive maneuvers once an aircraft has been detected, they are not considered a significant operational forecast problem.

The second, and most operationally important, type of contrail forms in the wake of an aircraft due to the engine exhaust's interaction with the environment. The combustion of aviation fuel results in the addition of water vapor to the atmosphere,

increasing the relative humidity of the wake and promoting contrail formation, and heat, which lowers the relative humidity and inhibits contrail development (Appleman, 1953:14). When these two competing processes result in the saturation of the air in the wake (the water vapor mixing ratio exceeds the saturation mixing ratio), a contrail will form (Coleman, 1996:3). This condition is possible only at the extremely low temperatures (usually less than -40 degrees Celsius) typical of the upper atmosphere. The exact temperature at which this condition is met is known as the *critical temperature*, or the temperature below which contrails will always form. The critical temperature depends on the ambient pressure, relative humidity, the amounts of heat and water vapor released from the engine, and on the mixing and particle formation processes in the aircraft's wake (Schumann, 1996b:4).

The need for an accurate method to forecast the occurrence of contrails has been recognized since the beginning of World War II. Although basic rules of thumb for avoiding contrail formation were developed during this period, accurate methods for predicting contrail layers were not developed until the late 1940s and early 1950s. The fundamental approach developed by Herbert Appleman in 1953, which will be discussed in Chapter 2, is still the basis for the contrail forecast method in use at the Air Force Global Weather Center (AFGWC) today. However, in 1989, the United States Air Force Strategic Air Command (SAC) expressed concern over the accuracy of contrail forecasts given to SAC aircrews (Peters, 1993:1). This concern led to a reinvestigation of the problem and modern research yielded new methods, or refinements to old ones, for forecasting contrail occurrence. The problem investigated in this thesis is an examination

of contemporary contrail forecast techniques, with an emphasis on performance in low environmental relative humidity conditions (where contrails are more difficult to forecast).

1.2 Problem Statement

Does the algorithm developed by Hanson and Hanson (Hanson and Hanson, 1995:2400) perform better than classical theory under low ambient relative humidity conditions? Does the forecast technique developed by Schumann (Schumann, 1996b:4) perform better than the method currently in use at AFGWC?

1.3 Significance of the Problem

The distinctive exhaust contrail clearly indicates the actual or recent presence of aircraft (Coleman, 1996:1). As a result, the formation of contrails is a detriment to mission accomplishment and aircrew survivability since contrails aid the enemy in the visual detection of aircraft. Contrails enhance the enemy's ability to direct anti-aircraft fire or vector defending fighters to intercept friendly formations. Persistent contrails, those that remain visible for a long period after formation, mark ingress and egress routes and provide the enemy an estimate of the number of aircraft on an mission. By revealing the configuration of the engines, contrails also give the enemy an indication of aircraft type. In addition to aiding the defender, contrails can also hinder the offensive force. Persistent contrails can spread and form large cirrus cloud layers which hinder the rendezvous of aircraft and make air-to-air refueling difficult (AWS/TR-81/001,1981:2).

The ease with which aircraft can be tracked by their contrails was most evident during World War II. High-altitude bomber formations, especially over Europe, were

3

easily located by the presence of their contrails. In some cases, pursuing German fighters would merely have to locate a contrail and follow it directly to an invading aircraft. As the war progressed, camouflage painting of American bombers and fighters was discontinued because it saved weight and did little to conceal an aircraft producing a long contrail. Today, the problem of contrail formation is even more important since stealth aircraft have become operational. Stealth bombers and fighters are just as easy to detect as conventional aircraft when they produce contrails, even at night.

Earlier forecast techniques proved satisfactory predicting contrails in relatively moist conditions. However, it was noted that theoretical predictions tended to disagree with contrail observations taken in dry environments (Hanson, 1995:2400). With the United States' continuing involvement in air operations over the Middle East, the need for an accurate dry environment contrail forecast algorithm has taken on new importance. The prevention of contrails is even more important when engaging a less sophisticated enemy who relies primarily on visually-guided weapons, as is often the case in this region.

1.4 The Benefit from Solving the Problem

Accurate contrail forecasts enhance mission accomplishment and aircraft survivability. With a precise contrail forecast, mission planners are able to route aircraft around areas likely to produce contrails or determine the best flight level to avoid their formation. Similarly, given a correct forecast, pilots who begin producing contrails would have the necessary information to either climb or descend to altitudes less likely to induce contrail formation.

4

1.5 Scope

1.5.1 Algorithms Tested.

Two new methods to forecast contrails were tested in this study, one developed by Hanson (Hanson and Hanson, 1995:2400) and the other developed by Schumann (Schumann, 1996b:4). These, in turn, were compared to the contrail forecast technique developed by Schrader, currently in use at AFGWC (Schrader, 1994:2). An explanation and derivation of each method will be discussed in subsequent chapters.

1.5.2 Parameters Varied.

The formation of contrails depends upon a number of variables, some associated with the aircraft, others with the atmosphere. One of the most important atmospheric variables is the relative humidity.

1.5.2.1 Relative Humidity.

The ambient relative humidity was varied in two ways. First, the relative humidity assumption of 40 percent in the troposphere, 70 percent within 300 meters of the tropopause, and 10 percent in the stratosphere was used to determine the critical temperatures (Bjornson, 1992:9). This method for determining the ambient relative humidity is currently in use at AFGWC to predict contrails for operational Air Force units. Calculations were then performed using in situ (ambient) relative humidity, as measured by a radiosonde with a very accurate moisture sensor. The difference in prediction skill score for each forecast method was then noted, using both relative humidity measurement techniques. Ambient relative humidity values were particularly useful in testing the Hanson algorithm (at low relative humidity) because it was suspected

that the 40/70/10 percent assumption greatly overestimated the true relative humidity profile. Since the purpose of this investigation was to examine the Hanson model's behavior under dry conditions, inflated moisture values would have been of no benefit.

1.5.3 Data Used.

Two datasets were used to evaluate the forecast methods under study. The first database consists of 98 contrail observations taken by the author and members of the 88th Weather Squadron at Wright-Patterson Air Force Base (WPAFB) in Dayton, Ohio. The second consists of 501 contrail observations taken as part of a flight test program by the Northrop Corporation at Edwards Air Force Base, California. The methods used to collect both sets of data will be discussed in Chapter 3.

1.6 General Approach

This research consists of three main parts: data collection, data processing, and statistical analysis of the results. The basic data consists of aircraft (contrail) observations coupled with the corresponding ambient temperature and relative humidity at flight level. This information was gathered either by aircrews (Edwards AFB data) or by launching radiosondes and observing commercial aircraft contrails (WPAFB data).

Data analysis consisted of inputting observed data (flight level pressure, ambient relative humidity, and the appropriate contrail factor) into the forecast algorithms, and obtaining a critical temperature for contrail formation. This temperature was then compared to the ambient temperature and a contrail forecast was made (contrails were forecast when the ambient temperature was colder than the critical temperature). For each forecast event, it was noted whether or not the aircraft actually produced a contrail at

6

the observed flight level. Using this process, a contingency table (discussed in Chapter 3) for all possibilities of contrail forecasts and occurrence was constructed for each new method, as well as for the AFGWC reference method.

Statistical measures of accuracy, bias, and skill were then computed from the contingency tables. Based on these statistics, forecast models were compared. In addition, computations using variable relative humidity values were also compared, focusing specifically on the Hanson algorithm.

1.7 Summary of Key Results

The Hanson forecast algorithm performed well under moist atmospheric conditions but became increasingly inaccurate as the ambient relative humidity approached lower values. In addition, the Schumann method was found to be statistically equivalent to the AFGWC method under almost all circumstances and did not suffer a decrease in performance as drier ambient conditions were tested.

1.8 Thesis Organization

Chapter 2 presents a brief discussion of past and present literature bearing directly upon the problem under investigation. It spans the first fundamental work of Appleman to the contrail forecast method published by Schumann in 1996.

Chapter 3 summarizes the basic thermodynamic theory of contrail formation and explains how contrails can be forecast. It also describes the equipment used to gather the contrail observations and how the data were collected. Finally, an overview of the data processing procedure is given.

Chapter 4 describes the data used to test each forecast method and the statistical tools employed to evaluate the results.

Finally, Chapter 5 presents the results of the statistical analysis and gives the conclusions one may make based on this data alone. In addition, operational recommendations and suggestions for further research are given.

2. Literature Review

2.1 Early Work

Aircraft first reached the high altitudes necessary to form contrails during the period 1914-1919 (Schumann, 1996b:4). Whereas the first contrail observations generated great curiosity, serious contrail research was not undertaken until World War II, when the tactical disadvantage of producing vapor trails was recognized. Many theories were put forth as to their origin, primarily by the British and Germans, but significant progress toward understanding contrail formation did not take place until the problem was examined using thermodynamic theory in the late 1940s.

2.1.1 Appleman, 1953.

Appleman devised the first thermodynamic explanation for the formation of contrails by jet aircraft. His calculations were based on three fundamental assumptions that form the basis for modern contrail theory (Appleman, 1953:20):

1. The wake behind the aircraft must be saturated with respect to water before any of the vapor in the exhaust gases can be transformed into visible water droplets.

2. The water droplets which form will freeze instantaneously, and the excess vapor in the trail will deposit onto the embryonic ice particles until the relative humidity in the wake is reduced to approximately 100 percent with respect to ice.

3. A solid water content of 0.004 gm m^{-3} is required for a "faint trail" and 0.01 gm m^{-3} for a "distinct trail."

Using these assumptions, a critical environmental temperature exists such that the passage of an aircraft will saturate its wake and produce a contrail.

Appleman's computations were based on the ratio of moisture increase to temperature increase of the environment due to the engine's exhaust, a ratio known today as the *contrail factor*. He determined this ratio to be 0.0336 g kg^{-1} C^{-1} for the jet engines of the period (non bypass engines). This engine characteristic was assumed to be constant and applicable to every jet aircraft under all operating conditions. Consequently, any aircraft with jet engines would raise the mixing ratio of its wake 0.0336 g kg^{-1} for each degree of temperature increase caused by the engine. Depending upon the initial conditions of the environment (i.e. the ambient temperature and relative humidity), and the degree of mixing between the exhaust and the entrained air, an aircraft would either saturate its wake (produce a contrail) or leave it unsaturated by its passage (Appleman, 1953:15).

Appleman described the formation of a contrail as a threefold process. First, the water vapor from the exhaust must raise the relative humidity of the wake to 100 percent with respect to water. Next, additional water vapor from the exhaust produces liquid droplets, which freeze instantaneously, and air which was saturated with respect to water is now supersaturated with respect to ice. Finally, the excess water vapor in the wake sublimes, allowing the ice crystals to grow until a final relative humidity of approximately 100 percent is reached with respect to ice. Using his contrail factor, Appleman was able to employ graphical techniques to determine critical temperatures for contrail formation from 1000 to 100mb, for various initial environmental conditions.

2.1.2 Appleman, 1957.

Appleman pointed out the major limitation to his forecast method was obtaining accurate high altitude, low temperature relative humidity measurements (Appleman, 1953:20). In the absence of reliable data, he recommended using a relative humidity of 70 percent near the tropopause and in high-cloud layers, and 40 percent at all other times (AWS TR 105-145, 1957:16). This assumption was later refined to 40 percent in the troposphere, 70 percent within 300 meters of the tropopause, and 10 percent in the stratosphere (Bjornson, 1992:9). The 40/70/10 percent assumption is still used today at AFGWC for operational contrail forecasting.

2.2 Recent Work

Modern contrail research has focused on explaining the occasional discrepancies between contrail observations and theoretical predictions using the Appleman method.

2.2.1 Peters, 1993.

Peters updated the work of Appleman to account for advancements in aircraft powerplant design. Whereas Appleman's contrail factor of $0.0336 \text{ g kg}^{-1} \text{ C}^{-1}$ was accurate for early jet engines, it isn't representative of today's bypass turbofan engines (Peters, 1993:5).

A bypass turbofan uses a portion of the energy from the combustion process to turn the engine's turbofan. Since part of the energy is not used to propel the aircraft, less energy (heat) is released into the wake (ΔT is reduced) and the contrail factor has a larger numerical value, all other conditions being equal, than for a non bypass engine (the engine type Appleman worked with). In addition, the turbofan flow tends to dilute the

resultant water vapor concentration in the exhaust (Δw is reduced), decreasing the contrail factor's value compared to a non bypass engine, all other conditions being equal (Schrader, 1994:4). Aircraft engines in use today may be conveniently classified as non bypass, low bypass, and high bypass.

Peters calculated a contrail factor for each engine type using typical exhaust pipe moisture and temperature readings under a variety of operating conditions (Peters, 1993:13). Since that time, extensive flight testing by the Northrop Corporation has resulted in more accurate contrail factors as shown in Table 1 (Schrader, 1994:4).

Table 1. Engine Contrail Factors (Schrader, 1994:4)

Engine Type	Contrail Factor $(g\ kg^{-1}\ C^{-1})$
Non Bypass	0.030
Low Bypass	0.034
High Bypass	0.039

2.2.2 Schrader, 1994.

Schrader developed the contrail forecast method currently in use at AFGWC which is used as the comparison reference for this study. His formulation is an updated version of Peters (1993) with Northrop's contrail factors and corrections to calculations under subsaturated conditions.

Schrader's corrections are twofold. First, whereas Peters calculates critical temperatures using the saturation vapor pressure with respect to ice, Schrader declares that calculations should be performed with respect to water since the vapor in the exhaust

passes through the liquid phase before freezing (Schrader, 1994:5). In addition, Schrader points out the inaccurate assumption used by Peters to interpolate critical temperatures for relative humidity between zero and 100 percent. Instead of assuming a linear relationship between the relative humidity and temperature, which is incorrect, Schrader uses the linear dependence of vapor pressure on temperature (Rogers and Yau, 1994:12) to calculate critical temperatures for intermediate relative humidity values (Schrader, 1994:8-9).

2.2.3 Hanson and Hanson, 1995.

Like Schrader, Hanson attempts to improve the basic Appleman method, as modified by Peters, to account for discrepancies between empirical data and theoretical computations at low relative humidity and high altitudes (lower pressures). Hanson uses the most current contrail factors, as shown in Table 1, and takes an alternative approach to finding critical temperatures for a relative humidity below 100 percent (Hanson and Hanson, 1995:2400-2402).

Like others, Hanson points out the inaccuracy of linearly extrapolating critical temperatures for subsaturated conditions from the 100 percent relative humidity value. He supports his argument by noting that previous derivations of the Appleman method are in good agreement with contrail observations for saturated conditions, but become increasingly less accurate as the relative humidity approaches lower values (Hanson and Hanson, 1995:2402).

Hanson calculates critical temperatures for subsaturated conditions by considering the mass of water vapor per unit volume involved in the mixing process. First, he

calculates the mass of water vapor present at the reduced relative humidity (with respect to the critical temperature under saturated conditions). From this, he determines the point on the saturation vapor pressure curve where this amount of water vapor would result in saturation. The lowest temperature where this condition is satisfied is the critical temperature for contrail formation at the reduced relative humidity (Hanson and Hanson, 1995:2402). Interestingly, critical temperatures for a dry atmosphere (relative humidity equal to zero percent) cannot be obtained using this method since a singularity would result. However, Hanson claims that such critical temperatures would be so low as to not be characteristic of the portion of the atmosphere under consideration (Hanson and Hanson, 1995:2403).

Using empirical data collected in the 1950s (AWS/TR-81/001, 1981:9), Hanson claims his method offers increased accuracy at lower relative humidity values. In addition, he points out the sensitivity of his formulation to relative humidity, and states the usefulness of the algorithm may be improved by using more precise relative humidity measurements (Hanson and Hanson, 1995:2404). In part, this research explores the performance of the Hanson method under dry conditions using very accurate relative humidity measurements.

2.2.4 Saatzer, 1995.

Part of the data (Edwards AFB data) used to test the Hanson and Schrader algorithms was gathered as part of a flight test program conducted by the Northrop Corporation in 1992 and 1993. The collection method and summary of the Edwards AFB data are described in Chapters 3 and 4, respectively. Unfortunately, not enough

information was available from these flights to calculate propulsion efficiencies (described below), so the Schumann method could not be tested using this data.

2.2.5 Schumann, 1996b.

Schumann has conducted extensive contrail research, primarily studying their effect on cloudiness and the global radiation budget. His paper reexamines the thermodynamic theory of contrail formation and attempts to explain the occasional discrepancies between predicted and observed critical temperatures for contrail development (Schumann, 1996b:4).

Schumann's theoretical explanation is based on the classic Appleman mixing cloud theory, except he considers the fraction of combustion heat dissipated as kinetic energy in the aircraft's trailing vortex system. This fraction of energy may be taken into account by using the propulsion efficiency (η) of the aircraft. The propulsion efficiency is a measure of the amount of work performed against drag forces to propel the aircraft, which is a small portion of the total energy (heat) of combustion. Incorporating the propulsion efficiency into the equations increases the accuracy of the critical temperatures, similar to accounting for the bypass ratio of the engine. Schumann shows that, by considering kinetic energy conversion using the propulsion efficiency, one may explain the contrails observed at ambient temperatures significantly above those predicted by the basic Appleman theory (Schumann, 1996b: 8).

Schumann estimates critical temperatures for relative humidity values between zero and 100 percent using a Taylor's series expansion (Schumann, 1996b:18). By expanding about the point where the engine mixing line is tangent to the saturation vapor

pressure curve (where the critical temperature for 100 percent relative humidity occurs), approximate critical temperatures may be obtained that are in good agreement with those obtained by Schrader as shown in Appendix B.

2.2.6 Schumann, 1996a.

Schumann published comments on the Hanson forecast method in the Journal of Applied Meteorology as this research was drawing to a close. He states how the Hanson method is equivalent to the classical (Appleman) approach when the atmosphere is saturated, but departs from classical theory as the atmosphere becomes drier. In fact, the critical temperature for contrail formation predicted by the Hanson algorithm approaches minus infinity as the relative humidity goes to zero. Classical theory predicts finite critical temperatures even for perfectly dry air (Schumann, 1996a:2283).

In addition, Schumann notes that Hanson gives no physical reasoning for the departure from classical theory when predicting critical temperatures for subsaturated conditions. In his comments, Schumann gives an example where the Hanson critical temperature is more than three degrees Celsius below the ambient temperature at which a contrail was observed (Schumann, 1996a:2284). Likewise, this thesis confirms many instances where Hanson's critical temperature in a dry environment was inaccurate and well below the temperature correctly predicted by the other methods. As will be shown, ambient temperatures much greater than that predicted by the Hanson method were recorded in the presence of contrails.

3. Methodology

3.1 Theory

Contrails form when water vapor in the exhaust gases, liberated by the burning of hydrocarbons, mixes with and saturates the aircraft's wake. Several factors determine whether or not a contrail will form for a given situation. Environmental factors include the pressure at which the aircraft is flying and the ambient temperature and relative humidity (with respect to water) of the atmosphere. The primary aircraft parameter is the contrail factor, or ratio of exhaust moisture to combustion heat (a function of the engine type) added during the mixing process. These variables can be related, and contrail forecasts made, by using simple mixing cloud theory.

3.1.1 Mixing Cloud Theory.

In the absence of heat losses or additions to the system (i.e. through radiational heating or the expansion of expelled gases under variable exhaust pressures), contrail formation is adiabatic and isobaric (Schumann, 1996b:9). Therefore, this process may be represented on a hygrometric chart (vapor pressure versus temperature).

The ambient air and exhaust gases, both at the same pressure p, may be depicted as points on this chart, as shown in Figure 1. Let the mass of exhaust gases be represented by point one on the diagram with mass M_1, temperature T_1, and specific humidity q_1. Let the environmental air be represented by point two, with mass M_2, temperature T_2, and specific humidity q_2. Next, assume both samples of air are mixed thoroughly under isobaric conditions (Rogers and Yau, 1994:44).
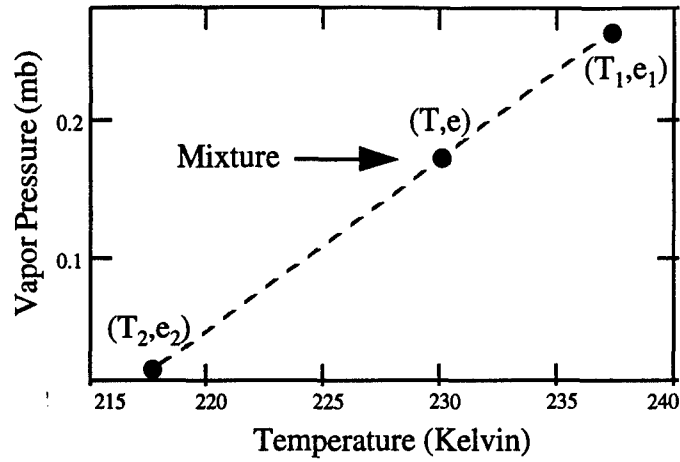
Figure 1. Mixture of Exhaust Gases and Ambient Air

After mixing, the specific humidity of the wake is a mass-weighted average of the specific humidities of the ambient air and the exhaust gases:

$$q \approx \frac{M_1}{M_1 + M_2} q_1 + \frac{M_2}{M_1 + M_2} q_2 \qquad (1)$$

Since

$$q \approx \varepsilon \frac{e}{p} \qquad (2)$$

where

$\varepsilon = 0.622$

e = vapor pressure (mb)

p = flight level pressure (mb)

it follows that the vapor pressure of the mixture is also a mass-weighted average of the individual vapor pressures (Rogers and Yau, 1994:44):

$$e \approx \frac{M_1}{M_1 + M_2} e_1 + \frac{M_2}{M_1 + M_2} e_2 \qquad (3)$$

Since it is assumed that contrail formation is an adiabatic process, no net gain or loss of heat will occur in the system during mixing. Therefore, the amount of heat gained by the environmental air will equal the amount of heat lost by the exhaust gases:

$$M_1(c_p + w_1 c_{pv})(T_1 - T) = M_2(c_p + w_2 c_{pv})(T - T_2) \qquad (4)$$

where

c_p = specific heat of dry air at constant pressure (J deg^{-1} kg^{-1})

c_{pv} = specific heat of water vapor at constant pressure (J deg^{-1} kg^{-1})

w_1 = mixing ratio of the exhaust gases (g kg^{-1})

w_2 = mixing ratio of the environmental air (g kg^{-1})

T = equilibrium temperature of the mixture (deg)

Since the mixing ratios are very small compared to the other terms in Equation (4), they may be neglected and we have:

$$T \approx \frac{M_1}{M_1 + M_2} T_1 + \frac{M_2}{M_1 + M_2} T_2 \qquad (5)$$

Therefore, like the vapor pressure, the temperature of the mixture is just a mass-weighted mean of the temperatures of the two constituents (Rogers and Yau, 1994:44).

Equations (3) and (5) imply that the temperature and vapor pressure of the mixture (aircraft's wake) lies approximately along a straight line connecting the two points on the hygrometric chart. The temperature and vapor pressure of the mixture depends upon the ratio of M_1 to M_2. If M_1 is greater than M_2, the coordinates of the mixture will lie closer to M_1 with respect to the midpoint of the line, as shown in Figure 1 (Rogers and Yau, 1994:45).

Since the saturation vapor pressure curve is simply a function of temperature according to Equation (6), the Clausius-Clapeyron equation, it may be represented on the hygrometric chart as the locus of points where the relative humidity equals 100 percent (Wallace and Hobbs, 1977:93-95).

$$\frac{de_s}{dT} = \frac{L}{T(\alpha_2 - \alpha_1)} \tag{6}$$

where

$\dfrac{de_s}{dT}$ = derivative of saturation vapor pressure with respect to temperature (Pa K^{-1})

L = latent heat of vaporization (J kg^{-1})

α_2 = specific volume of the vapor state at temperature T (m^3 kg^{-1})

α_1 = specific volume of the liquid state at temperature T (m^3 kg^{-1})

Any temperature, vapor pressure pair lying above the curve (see Figure 2) represents a supersaturated condition, while any point below the curve is subsaturated.
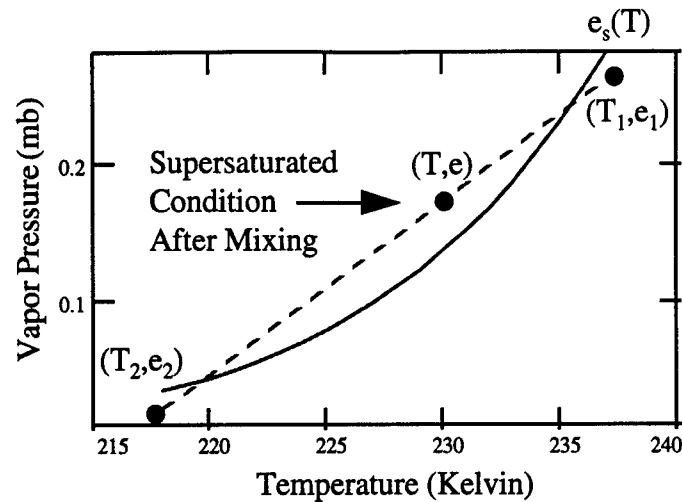
Figure 2. Necessary Condition for Contrail Formation

Superimposing the saturation vapor pressure curve over the mixing line allows

one to determine whether the aircraft's wake will be supersaturated after mixing. If the

coordinates of the mixture (T,e) lie above the saturation vapor pressure curve, the wake is

supersaturated and a contrail will form (see Figure 2). Determining whether a contrail

will form depends on accurately predicting the state of the atmosphere (point two on the

chart) and the characteristics of the exhaust gases (point one).

3.1.2 Forecasting Contrail Formation.

In addition to illustrating how contrails form, the hygrometric diagram may also

be used to predict their occurrence. In order to predict contrails, one must first be able to

determine the engine's contrail factor.

21

3.1.2.1 Contrail Factor.

The contrail factor ($\Delta\omega/\Delta T$) may be determined by taking the ratio of water to heat added to the atmosphere by the combustion process (Schrader, 1994:3-4):

$$\frac{\Delta\omega}{\Delta T} = \frac{\dfrac{M_{H_2O}}{M_{ex}N}}{\dfrac{H_f}{M_{ex}Nc_p}} = \frac{M_{H_2O}c_p}{H_f} \tag{7}$$

where

ω = mixing ratio (g kg^{-1})

$\dfrac{\Delta\omega}{\Delta T}$ = contrail factor (g kg^{-1} deg^{-1})

M_{H2O} = mass of water vapor produced per unit mass of fuel burned (g)

M_{ex} = mass of exhaust gas produced per unit mass of fuel burned (g)

N = ratio of ambient air to exhaust gas in the mixture

H_f = heat released per unit mass of fuel burned (J)

c_p = specific heat of air at constant pressure (J deg^{-1} kg^{-1})

As shown in Table 1, the contrail factor has been determined for the three most common types of engines in use on today's aircraft.

3.1.2.2 Critical Slope.

The contrail factor may be used to determine the *critical slope*, or slope of the line which passes through the point representative of the exhaust gases and tangent to the saturation vapor pressure curve. The critical slope is given by (Schrader, 1994:7):

$$\frac{\Delta e}{\Delta T} \approx \frac{p}{622} \frac{\Delta \omega}{\Delta T} \qquad\qquad (8)$$

where

$\dfrac{\Delta e}{\Delta T}$ = the slope of the line passing through the engine conditions tangent to the

saturation vapor pressure curve (mb deg^{-1})

The critical slope is illustrated in Figure 3.
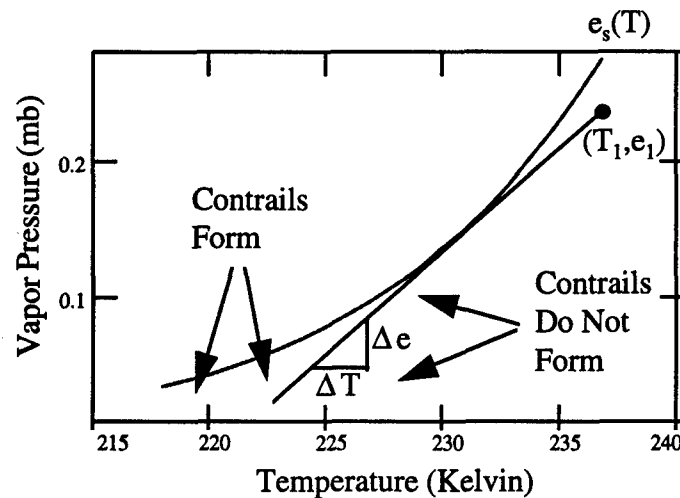
Figure 3. Saturation Vapor Pressure Curve and Critical Slope

23

This line, with slope $\frac{\Delta e}{\Delta T}$, represents a set of critical temperatures as a function of environmental relative humidities. For environmental conditions lying to the left of this line, mixing of the ambient air with the exhaust gases will lead to supersaturation of the wake since the mixing line would intersect the saturation vapor pressure curve. For environmental conditions to the right of the line, contrails will not form (Schrader, 1994:2).

The line tangent to the saturation vapor pressure curve may be used to determine the critical temperature for contrail formation when the environment is saturated with respect to water (relative humidity equals 100 percent). The critical temperature (T_C) is found by simply calculating the temperature at the point of tangency. Any ambient temperature colder than T_C will produce contrails when the environmental relative humidity is 100 percent. For a relative humidity below 100 percent, the critical temperature is determined by finding the temperature at the point where the *critical line*, for that relative humidity, first crosses the saturation vapor pressure curve on the left. Any temperature colder than T_C will lead to contrail formation. Critical lines and temperatures for 100 and 10 percent relative humidity, as shown in Figure 4, were computed using the Schrader method at 500 mb using Equations (11) and (12).

3.2 Equipment

Research-quality radiosondes were used to measure profiles of atmospheric parameters during contrail data collection at Wright-Patterson AFB. Although National Weather Service upper air data were available every twelve hours from Wilmington, Ohio (26 miles away), it was not used because it would be six hours old at observation time. In addition, the relative humidity values would not have sufficient resolution for contrail observation purposes since most of the radiosondes in common use today can only measure relative humidity in the 15 to 100 percent range (Brock and Nicolaidis, 1985:6-9). Therefore, accurate relative humidity measurements for the Dayton area could only be obtained by launching research-quality radiosondes from Wright-Patterson AFB. Sensors
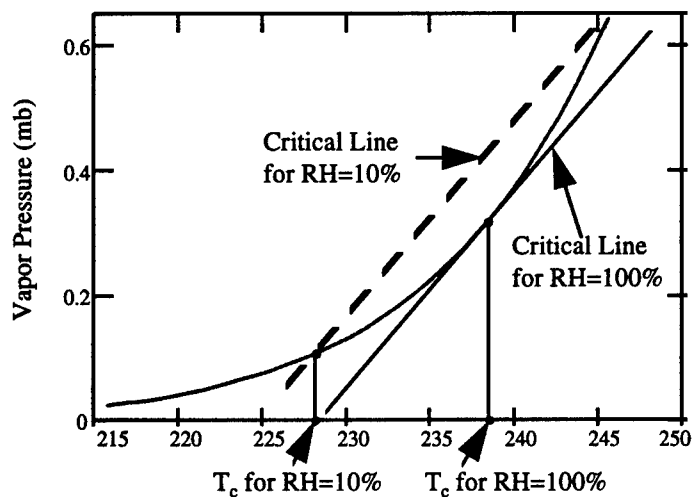
Figure 4. Critical Temperatures for Contrail Formation

used in the Northrop study were aircraft-mounted and will be discussed separately.

3.2.1 Equipment Used to Gather WPAFB Data.

Radiosondes manufactured by Vaisala and Atmospheric Instrumentation Research, Inc. (A.I.R., Inc.) were used to gather accurate upper air data prior to recording contrail observations. All launches were conducted with either 100 or 200 gram balloons using the operating manual's standard setup and launch procedures. Most launches used Vaisala radiosondes since they were available in the greatest quantity.

A standard Vaisala RS80 model radiosonde with pressure, temperature, and humidity sensors was used. The RS80 series sonde uses a capacitive BAROCAP® pressure sensor, a THERMOCAP® temperature sensor, and a HUMICAP® humidity sensor. The HUMICAP® uses a capacitance thin film humidity sensor with excellent long-term stability and a reliable response at low temperatures and after passing through clouds. All parameters were measured approximately every 1.5 seconds. See Table 2 for technical data regarding each sensor (J. Polander, 1996, personal communication).

Table 2. Vaisala RS80 Technical Data

	Pressure	Temperature	Relative Humidity
Measuring Range	1060 to 3mb	+60 to -90° C	0 to 100 % RH
Resolution	0.1mb	0.1° C	1 % RH
Accuracy: Reproducibility Repeatability	 0.5mb 0.5mb	 0.2° C up to 50mb 0.2° C	 < 3 % RH 2 % RH
Lag	Not Available	< 2.5 s (6 m s^{-1} flow at 1000 mb)	1 s (6 m s^{-1} flow at 1000mb, +20° C)

A.I.R., Inc. GPS-700 radiosondes were used when the supply of Vaisala sondes was exhausted. Similar to the Vaisala, the GPS-700 uses an aneroid capacitance transducer to measure pressure, a Negative Temperature Coefficient bead thermistor to measure temperature, and a HUMAIR™ capacitive sensor to measure relative humidity. The HUMAIR™ sensor provides accurate measurements in clouds and in very cold and dry conditions. All parameters were measured once each second. See Table 3 for data regarding sensor performance (J. Polander, 1996, personal communication).

As shown in Tables 2 and 3, each radiosonde system was capable of measuring the upper atmosphere accurately and quickly enough to provide high resolution input into the three contrail forecast methods under consideration.

Table 3. A.I.R., Inc. GPS-700 Technical Data

	Pressure	Temperature	Relative Humidity
Measuring Range	1050 to 5mb	+50 to -90° C	0 to 100 % RH
Resolution	0.1mb	0.01° C	0.1 % RH
Accuracy	1mb	0.3° C	3 % RH
Response Time	< 0.1 s	< 1 s	< 1 s
Hysteresis	Not Available	Not Available	< 1 % RH

3.2.2 Equipment Used to Gather Edwards AFB Data.

Northrop used aircraft-mounted sensors to measure the in-situ pressure, temperature, and dewpoint (from which relative humidity was derived). The T-33 aircraft was equipped with two sets of temperature and dewpoint sensors for comparison purposes - an OPHIR Corporation infrared radiometric thermometer and hygrometer (also present on the Lear 35 chase plane), and a conventional Rosemount thermometer and

chilled mirror hygrometer. In addition, weather balloon measurements of temperature

and relative humidity were obtained from the Naval Weapons Center at China Lake,

California to validate the T-33 sensor readings (Saatzer, 1995: 1-1,4-5).

Since the OPHIR thermometer was generally found to be inaccurate, the

conventional thermometer was used for all ambient temperature measurements and

dewpoint to relative humidity conversions (Saatzer, 1995:6-16).

The chilled mirror hygrometer was the primary sensor measuring the

dewpoint/frost point temperatures. However, on almost every flight, this instrument

suffered from not stabilizing rapidly enough for changing humidity conditions, and

accumulating moisture in the instrument housing. These two effects combined to

produce an abnormally high (over 100 percent) relative humidity on many occasions. The

OPHIR hygrometer performed well intermittently but, like the chilled mirror hygrometer,

could have been improved with a more tailored installation. Overall, the relative

humidity was measured with a probable absolute uncertainty of ± 15 percent. The

temperature and pressure altitude were subject to uncertainties of ± 0.45°C and ± 200 feet

respectively (Saatzer, 1995: 6-14,6-15,8-1).

3.3 Data Collection Procedure

3.3.1 WPAFB Data.

Contrail observations were taken at Wright-Patterson AFB from 11 September to

17 October 1996. Because of bad weather and funding constraints, only 12 days were

available for balloon launches/observations.

3.3.1.1 Radiosonde Launches.

Radiosondes were prepared and released at approximately 1300 LT on days when weather conditions allowed contrail observations to be made. After launching and ensuring the telemetry was good, preparations were made for contrail observing as the balloon ascended to commercial aircraft flight levels. Once the balloon was at approximately 30 000 feet, observations of air traffic in the Dayton area sector were begun (see Figure 5).
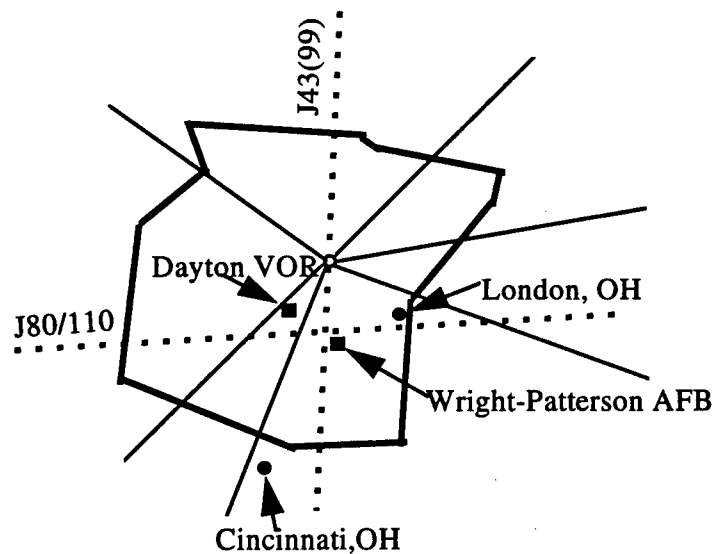
Figure 5. Sector 98 Super High (FL350 and Above)/Sector 88 High (Below FL350)

3.3.1.2 Contrail Observations.

Air traffic was observed using a small spotting telescope (45X magnification) and a reflector telescope (approximately 90X magnification). In addition, a VHF scanning radio was used to intercept communications traffic with Indianapolis Center, controlling

29

the sector 88/98 traffic. By using the reflector telescope, the aircraft type and color or airline logo could be observed, given a favorable side-viewing angle. Occasionally, radio calls would occur simultaneously with the visual observation, giving a possible airline, flight number, and current altitude or direction. For each aircraft, the following information was recorded:

1. Aircraft type.

2. Airline (if possible).

3. Time overhead, or closest to, our viewing position.

4. Direction of flight.

5. Nature of contrail (short-lived or evaporated quickly, persistent, none).

Most aircraft were observed flying the J80/110 or the J43/99 routes, as shown in Figure 5. In addition to aircraft observations, general sky conditions were documented for each day. An extract of the contrail log for 3 October 1996 is shown in Table 4.

Table 4. Extract of Contrail Log for 3 October 1996

Aircraft Type	Airline	Time	Direction	Contrail
MD 80/DC 9	American Airlines	13:23 L	Westbound/ Overhead	None
757/767	United Airlines	13:26 L	Westbound/Due South	Short-lived con
737	Southwest Airlines	13:47 L	Eastbound/Due North	None
Fokker/DC 9	US Air	14:12:30 L	Eastbound/Due North	None
Private Jet	N/A	14:20 L	Eastbound/Due South	Short-lived con

3.3.1.3 Upper Air Analysis.

After all contrail observations were completed, the radiosonde telemetry was analyzed using a computer algorithm. For each sounding, the following information was determined:

1. Pressure at standard flight levels (mb).

2. Ambient temperature at standard flight levels (°C).

3. Ambient humidity at standard flight levels (% RH).

4. Assumed humidity at standard flight levels (40/70/10 % RH).

5. Tropopause height (mb).

6. Tropopause temperature (°C).

7. ± 300 meters of tropopause height (mb).

The analysis for 3 October 1996 is shown in Table 5.

Table 5. Sounding Analysis for 3 October 1996

Flight Level (kft)	Pressure (mb)	Ambient Temperature (°C)	Ambient Relative Humidity (%)	Assumed Relative Humidity (%)
430	162.3	-62.6	10	10
410	178.6	-63.2	11	70
390	196.5	-61.0	12	40
370	216.3	-58.4	12	40
350	238.0	-54.7	11	40
330	261.6	-49.9	12	40
310	287.0	-44.7	11	40

Tropopause +300m height = 167.9mb
Tropopause height = 176.0mb, Temp = -63.6°C
Tropopause -300m height = 184.5 mb

3.3.1.4 Federal Aviation Administration Flight Log Comparison.

Once all of the information had been gathered locally, a request was sent to the Federal Aviation Administration (FAA) office in Indianapolis, Indiana for a copy of the flight log for the day's sector 88/98 traffic. An extract from the sector 98 log for 3 October 1996 is shown in Table 6. The log provides the aircraft identification (AID), the time of entry into and exit from sector 98 airspace, the aircraft (AC) type, the flight plan (FP) type, the flight plan (origin to destination), and the altitude (ALT) at which the aircraft transited the sector (in thousands of feet).

Since all of the aircraft we observed were operating in an FAA Positive Control Area, they were equipped with automatic pressure altitude reporting equipment. By Federal Aviation Regulations, this equipment must be calibrated to within 125 feet of the flight level indicated by the altimeter in the cockpit (set to a standard pressure of 29.92 inches of mercury). Therefore, the maximum uncertainty in the altitudes provided by the FAA is 125 feet (Federal Aviation Regulations, 1990:91-39,91-40).

Table 6. Extract of FAA Flight Log for 3 October 1996 (Sector 98)

AID	ENTRY TIME	EXIT TIME	AC TYPE	FP TYPE	FLIGHT	PLAN	ALT
TWA279	1716	1738	DC9	OVER	EWR	TO STL	FL350
UAL57	1722	1749	B757	OVER	IAD	TO SFO	FL350
USA298	1726	1738	FK10	OVER	MCI	TO PHL	FL330
AAL2075	1744	1749	B757	OVER	YYZ	TO DFW	FL350
USA754	1802	1815	DC 9	OVER	STL	TO PIT	FL330
AWE255	1804	1824	EA320	DEPT	CMH	TO LAS	FL350
N1526L	1809	1819	C650	OVER	SUS	TO BWI	FL410

By matching the observations from our record (see Table 4) with the FAA log, the altitude of each observed aircraft could be accurately determined. The process of matching a local aircraft observation with a FAA log entry involved the following steps:

1. Aircraft in sector 88/98, according to the FAA record, during the time of observation were identified. Since we recorded the time the aircraft was overhead or at its closest approach, and because Dayton is not on the edge of the sector, those aircraft that were just entering or leaving sector 88/98 at the time under scrutiny were eliminated from consideration.

2. From the origin and destination portion of the FAA log, those aircraft flying in the wrong direction from that observed were eliminated.

3. From the aircraft still under consideration as possible matches, the aircraft type and airline (if applicable) were compared.

4. Once a positive match was made, the altitude during sector transit was recorded. Only those aircraft that followed a flight plan overflying sector 88/98 (OVER) were considered, since aircraft arriving (ARRV) or departing (DEPT) would probably have not been at a constant altitude during our observation.

If any doubt existed about the quality of a match, it was eliminated from our database. Of the 154 aircraft observed, only 98 or 64 percent were positively matched up with aircraft in the FAA logs. It was not possible to match every aircraft with a log entry for a variety of reasons. On some occasions, aircraft of the same type and airline were transiting the airspace within the same approximate time period, making a positive match

difficult. However, the greatest problem was identifying similar private jets flying in the same direction at approximately the same time.

3.3.1.5 Data Combination.

Once the altitude of each aircraft in the observed database was determined, the atmospheric conditions at flight level were taken from the day's sounding analysis. In addition, the aircraft were identified as having either a high or low bypass engine, and the appropriate contrail factor or propulsion efficiency (Schumann method) was selected. When there was doubt about the engine type, a high bypass contrail factor was assumed. The complete database of WPAFB observations is contained in Appendix C.

3.3.2 Edwards AFB Data.

Contrail data from the Northrop study were collected as part of a test program at Edwards AFB, California from January 1992 to March 1993. Flight test procedures involved having a T-33 gradually climb to an altitude suitable for contrail formation, at which time a Lear 35 chase plane would drop below and behind the T-33 to observe contrail conditions. Once the chase plane was in place, the T-33 would continue to climb until observers detected the onset of contrail formation. After the contrail was well established, the T-33 would then descend to altitudes at which contrail formation was not possible. This cycle of contrail initiation and termination was repeated many times for each flight as atmospheric conditions and fuel constraints allowed (Saatzer, 1995:3-10-3-12).

Contrail conditions, as determined by observers in the chase plane, were divided into three categories: 0 (no contrail), 1 (visible onset), and 2 (well developed). Saatzer

points out the declaration of a visible contrail (category 1) is based on the best possible viewing angle and such a contrail would not be visible to a distant observer (i.e. on the ground). He defined this condition as an "invisible contrail."

An invisible contrail is one which has a solid water content less than 0.004 g m^{-3} (Saatzer, 1995:3-1). Since the Appleman requirement for visibility of 0.004 g m^{-3} was developed for detection by an observer on the ground, it did not apply to observers in the chase plane. Therefore, contrail onset was declared frequently when the ice crystal content was well below 0.004 g m^{-3} (Saatzer, 1995:3-1). Since contrail detection for an observer on the ground, and especially for a pilot in a pursuing enemy aircraft, is eminent under these conditions, all occurrences of category 1 contrails were treated as "yes" observations for the purposes of this study.

Although the contrail factor for the T-33 engine is constant under constant power conditions (≈ 0.030 g kg^{-1} C^{-1}), it changed during portions of the flight when engine power was used to change altitude rather than angle of attack. As a result, the contrail factor varied between 0.020 and 0.043 g kg^{-1} C^{-1} during the test program. When maneuvers requiring an engine power change were used, a new contrail factor was computed for each contrail observation (Saatzer, 1995:6-6). As an example, data for flight 626 is shown in Table 7.

Table 7. Data for Flight 626 (Saatzer, 1995:C-1)

Flight Number	Ambient Temperature (°C)	Ambient RH (%)	T-33 Altitude (ft)	Contrail Factor (g kg^{-1} C^{-1})	Contrail Status
626	-53.90	27.80	37060	0.027	1
626	-54.21	27.80	37235	0.028	2
626	-55.00	25.60	37610	0.036	2
626	-54.30	23.30	37360	0.036	1
626	-55.50	23.00	37960	0.030	1
626	-53.65	20.90	36960	0.037	0

3.4 Critical Temperature Equations

The three contrail forecast methods under consideration are based on the theoretical development outlined at the beginning of this chapter. However, each algorithm has variations which lead to different critical temperatures for the same pressure and relative humidity values.

3.4.1 Schumann Method.

Schumann calculates the critical slope of the mixing line ($\Delta e/\Delta T$) as a function of the propulsion efficiency of the aircraft (Schumann, 1996b:9):

$$G = \frac{EI_{H_2O}c_p p}{\varepsilon Q(1-\eta)}$$

(9)

where

EI_{H2O} = the emission index of water vapor for the fuel burned (kg kg^{-1})

c_p = the specific heat of air at constant pressure (J deg^{-1} kg^{-1})

p = the pressure at flight level (mb)

ε = 0.622 (unitless)

Q = the specific combustion heat of the fuel burned (MJ kg^{-1})

η = propulsion efficiency (unitless)

Propulsion efficiencies for high and low bypass aircraft are calculated in Appendix D.

Next, using the critical slope, the temperature at which the mixing line just touches the saturation vapor pressure curve is determined (T_c for RH=100 percent in Figure 4). This value is found by equating the derivative (with respect to temperature) of the saturation vapor pressure equation and the critical slope, and solving for the temperature at the point of tangency. The temperature where both slopes are equal is the critical temperature for contrail formation when the ambient relative humidity is 100 percent (Schumann, 1996b:10). Critical temperatures for zero percent relative humidity may be obtained explicitly; however, critical temperatures for intermediate relative humidity values are found by performing a Taylor series expansion about T_c for RH=100 percent (Schumann, 1996b:10,18).

3.4.2 Hanson Method.

Hanson calculates the critical slope of the mixing line by converting the contrail factor (g kg^{-1} C^{-1}) to units of vapor pressure per degree (mb C^{-1}) or

$$\frac{\Delta e}{\Delta T} = \frac{p(C_F)}{622} \tag{10}$$

where

C_F = the contrail factor (g kg^{-1} C^{-1})

Next, similar to the Schumann method, the critical temperature for saturated conditions is found by equating the critical slope to the saturation vapor pressure slope and finding the temperature for which the slopes are equal through an iterative process (Hanson and Hanson, 1995:2402).

Critical temperatures for subsaturated conditions are found by multiplying the slope of the saturation vapor pressure curve by the correction factor 100/RH and solving for temperature. It should be noted that critical temperatures for completely dry conditions (relative humidity equals zero percent) cannot be obtained from this method since a singularity would result (Hanson and Hanson, 1995:2402-2403).

3.4.3 Schrader Method.

Schrader uses the same basic approach as Hanson for saturated conditions. However, for unsaturated conditions, the methods differ significantly. First, since the vapor pressure is linear in temperature (not the relative humidity), the vapor pressure at the critical temperature for the given relative humidity is found by linear interpolation:

$$e(T_{c,RH}) = e_s(T_{c,100}) - (T_{c,100} - T_{c,RH})\frac{de_s}{dT}\bigg|_{T_{c,100}} \tag{11}$$

where

$e(T_{c,RH})$ = vapor pressure at given relative humidity (mb)

$e_s(T_{c,100})$= saturation vapor pressure at the critical temperature for 100 percent relative humidity (mb)

$T_{c,100}$ = critical temperature at 100 percent relative humidity (K)

$T_{c,RH}$ = critical temperature at given relative humidity (K)

$\left.\dfrac{de_s}{dT}\right|_{T_{c,100}}$ = derivative of the saturation vapor pressure curve, with respect to

temperature, evaluated at the critical temperature for saturated conditions (mb K^{-1})

Using the Goff-Gratch formula for saturation vapor pressure, and the definition of relative humidity in terms of vapor pressure and saturation vapor pressure, a relationship in terms of relative humidity and critical temperature can be found (Schrader, 1994:8-9):

$$\frac{e(T_{c,RH})}{e_s(T_{c,RH})} \times 100 = RH \qquad (12)$$

where

$e_s(T_{c,RH})$ = saturation vapor pressure at the given relative humidity value (mb)

RH = relative humidity (%)

This equation is then solved by an iterative process such that the critical temperature makes both sides of the equation equal (Schrader, 1994:9).

To illustrate the differences in the three methods, critical temperatures for standard pressure levels, relative humidities, and a high bypass contrail factor (propulsion efficiency) are shown in Appendix B. As can be seen, all methods produce nearly

identical results under saturated conditions. Under subsaturated conditions, the
Schumann and Schrader methods agree closely at all relative humidities. However, the
critical temperatures at low relative humidity, as calculated using the Hanson equations,
are significantly colder than those determined by the other two methods.

3.5 Data Processing

Theoretical critical temperatures for contrail formation were computed for each
observation as described in Appendix E. For each of the three methods under
consideration, the following variables were input into the equations:

1. Pressure at flight level (mb).

2. Relative humidity at flight level (% RH).

3. Contrail factor (g kg^{-1} C^{-1}) (Hanson and Schrader (AFGWC) methods only).

4. Propulsion efficiency (unitless) (Schumann method only).

Once a critical temperature for a specific flight level was calculated, it was
compared with the ambient temperature at flight level and a yes/no contrail forecast was
made. If the ambient temperature was colder than the critical temperature, contrails were
forecast to occur. If the ambient temperature was warmer than that required for wake
saturation, contrails were not forecast to occur.

After the contrail forecast was made, it was compared to the actual contrail
observation. By comparing the contrail forecast with the observation at each flight level,
the problem of comparing the contrail forecast methods was reduced to one of simple
categorical forecast verification.

3.5.1 Categorical Forecast Verification.

Categorical forecasts are those that consist of a statement, with no expression of uncertainty, that one and only one of a set of finite possible outcomes will occur. The predictands under these circumstances are discrete, meaning the observed variable can take on only one of a set of possible values. In this study, the forecast is simply a "yes/no" expression that contrails will or will not occur, and contrails are either observed (yes) or not observed (no). Such forecast verification problems are easily analyzed using a 2 x 2 *contingency table* (Wilks, 1995:238).

The 2 x 2 contingency table is a display of absolute frequencies, or counts, of the four possible combinations of forecast and event pairs. The contingency table used in this study is shown in Figure 6:

<div align="center">

Contrails Observed

		yes	no	
	yes	a	b	a+b
	no	c	d	c+d
		a+c	b+d	n

(Left axis label: Contrails Forecast)

</div>

Figure 6. 2 x 2 Contingency Table (Wilks, 1995:239)

The four possible forecast/event pairs are:

1. Contrails are forecast and are observed to occur (entry a).

2. Contrails are forecast but are not observed to occur (entry b).

3. Contrails are not forecast but observed to occur (entry c).

4. Contrails are not forecast and are not observed to occur (entry d).

Other information available from the table is the total number of contrails forecast (a+b), the total number of contrails not forecast (c+d), the total number of contrails observed (a+c), the total number of contrails not observed (b+d), and the sample size (a+b+c+d=n). Contingency table analysis will be discussed further in Chapter 4.

3.5.2 WPAFB Data Calculations.

Contingency tables were constructed for various perturbations of the WPAFB dataset to evaluate differences among the three methods under consideration. The following data and subsets of data were considered:

1. All observations (assumed relative humidity of 40/70/10%).

2. All observations (in-situ relative humidity).

3. High bypass engine observations (in-situ relative humidity).

4. Low bypass engine observations (in-situ relative humidity).

5. Daily observations (in-situ relative humidity).

3.5.3 Edwards AFB Data.

The Northrop Corporation observations were used to compare the Hanson and Schrader contrail forecast methods only, since engine parameters needed to compute the

propulsion efficiency using the Schumann method (thrust and specific fuel consumption) were not available.

4. Data Description and Analysis

4.1 Data Description

4.1.1 WPAFB Data.

The WPAFB database is composed of 98 observations taken over the course of 12 days. The altitude of aircraft observed ranged from flight level 310 (31 000 feet or 287mb in the standard atmosphere) to flight level 410 (41 000 feet or 179mb). Of all aircraft positively identified, 92 percent (90 of 98) were flying in the troposphere, four percent (4 of 98) were flying in the stratosphere, and four percent (4 of 98) were flying within 300 meters of the tropopause. A total of 75 of 98 aircraft (76.5 percent) were observed to produce either short-lived or persistent contrails. Ambient temperatures ranged from -63.7 to -42.9°C, and in-situ relative humidity ranged from 1 to 37 percent.

As stated in Chapter 3, subsets of the data, as well as the complete dataset, were analyzed in order to determine under which conditions each forecast method performed best. Each database was summarized by computing averages of the controlling parameters. The summary of WPAFB data is presented in Table 8. Average ambient temperature, average ambient relative humidity, and average assumed relative humidity are for flight levels 310 to 410.

4.1.2 Edwards AFB Data.

The Edwards AFB database is composed of 501 observations taken during 23 individual test flights. Observations span altitudes from 28 000 to 39 000 feet and contrail onset temperatures of -47 to -55° C. Relative humidity varied from 18 to 100

percent (Saatzer, 1995:ix). Since the Schrader method can only accommodate relative humidity values of less than or equal to 100 percent, supersaturated relative humidity values (obtained from inaccurate moisture measurements) were reduced to 100 percent for the purposes of this study. All relative humidity averages were also calculated with a 100 percent maximum value. A summary of the Edwards AFB data is presented in Table 9.

Table 8. Summary of WPAFB Data

Date or Type	Sample Size	Average Flight Level (mb)	Average Ambient Temp (°C)	Average Ambient RH (%RH)	Average Assumed RH (%RH)	Aircraft with Contrails (%)	Tropopause Height (mb)
All Days	98	232	-52.1	12	38	77	188
11 Sep 96	4	230	-49.0	8	40	50	164
19 Sep 96	9	204	-50.9	5	40	89	168
30 Sep 96	6	231	-51.6	8	40	100	159
2 Oct 96	4	213	-52.0	8	40	75	120
3 Oct 96	9	247	-55.3	12	45	56	176
4 Oct 96	29	234	-56.3	31	45	97	187
5 Oct 96	4	217	-54.8	25	40	75	204
7 Oct 96	10	239	-52.4	10	40	30	189
8 Oct 96	3	247	-47.3	6	20	33	281
11 Oct 96	8	236	-52.5	16	35	63	227
16 Oct 96	6	250	-51.0	9	30	67	249
17 Oct 96	9	229	-51.6	8	40	78	127
Low Bypass	28	250	-51.1	22	42	61	N/A
High Bypass	70	225	-54.4	17	39	83	N/A

4.2 Data Analysis

A perfectly accurate contrail forecast method would produce a 2 x 2 contingency table with zero entries along the lower-left to upper-right diagonal. Under these circumstances, all "yes" forecasts would be accompanied by observed contrails, and all "no" forecasts would accurately predict no observed contrails (Wilks, 1995:239-240). An example of a perfect forecast contingency table is shown in Figure 7. For imperfect forecasts, statistical measures of accuracy and skill are employed to distinguish between competing forecast methods (Wilks, 1995:240).

Contrails Observed

		yes	no	
Contrails Forecast	yes	a	b=0	a
	no	c=0	d	d
		a	d	n.

Figure 7. Contingency Table for a Perfect Forecast (Wilks, 1995:239)

Table 9. Summary of Edwards AFB Data

Flight Number	Sample Size	Average Flight Level (mb)	Average Ambient Temp (°C)	Average Ambient RH (%RH)	Average Contrail Factor (gkg^{-1}°C^{-1})	Aircraft with Contrails (%)
All Flights	501	265	-51.5	71	0.0283	74
625	13	235	-51.6	94	0.0299	85
626	6	213	-54.4	25	0.0323	83
627	2	198	-55.0	52	0.0280	100
628	14	210	-54.2	47	0.0267	71
629	7	241	-52.4	94	0.0276	86
630	2	212	-54.1	51	0.0415	100
632	28	233	-53.3	55	0.0250	79
633	36	233	-51.7	91	0.0250	72
635	20	280	-50.3	95	0.0286	75
636	18	267	-52.5	31	0.0257	72
637	20	248	-52.1	54	0.0303	75
639	31	218	-53.5	52	0.0303	81
640	30	264	-51.3	79	0.0303	77
642	42	242	-52.1	74	0.0295	76
643	30	286	-50.4	84	0.0310	73
646	26	296	-50.7	65	0.0285	65
648	21	287	-49.6	99	0.0270	76
649	44	294	-49.8	87	0.0282	70
652	20	289	-51.3	54	0.0282	75
653	21	283	-50.8	76	0.0276	71
655	26	304	-50.4	64	0.0277	73
656	26	303	-51.7	66	0.0277	65
660	18	284	-51.8	31	0.0281	78

4.2.1 Measures of Accuracy.

A measure of accuracy refers to the average agreement between forecasting a certain event and that event occurring (Wilks, 1995:236). Many measures of accuracy are available to summarize categorical "yes/no" forecasts.

47

4.2.1.1 Hit Rate (H).

The hit rate is a basic measure of accuracy and is the fraction of n forecasting opportunities when the forecast method correctly predicts the observed event. Referring to Figure 7, the hit rate is given by:

$$H = \frac{a+d}{n}$$ (13)

where

H = hit rate

a = contrails that were forecast and observed

d = contrails that were not forecast and were not observed

n = sample size

The hit rate credits correct "yes" and "no" forecasts equally. It also penalizes incorrect forecasts equally. The best possible hit rate is one, the worst possible is zero (Wilks, 1995:240).

4.2.1.2 Critical Success Index (CSI) or Threat Score.

An alternative measure of accuracy, the critical success index considers only those events where contrails were forecast (entries a and b in the contingency table) or observed (entry c). As such, it may be considered as the hit rate once all correct "no" forecasts have been eliminated from consideration. The critical success index is given by:

$$CSI = \frac{a}{a+b+c} \qquad\qquad (14)$$

where

b = contrails that were forecast and were not observed

c = contrails that were not forecast and were observed

The CSI is particularly effective when the number of "yes" forecasts is substantially

lower than the number of "no" forecasts. Like the hit rate, the best possible score is one,

and the worst possible score is zero (Wilks, 1995:240).

4.2.1.3 False Alarm Rate (FAR).

The false alarm rate gives the proportion of "false alarms" or those events that

were forecast but not observed. Mathematically, the false alarm rate is given by:

$$FAR = \frac{b}{a+b} \qquad\qquad (15)$$

Unlike the other measures of accuracy, the best possible FAR is zero, and the worst

possible FAR is one (Wilks, 1995:240-241).

4.2.2 Measure of Bias.

The bias ratio, for categorical forecast methods, is a comparison of the mean

forecast with the mean observation. It is simply the ratio of the number of "yes" forecasts

to the number of "yes" observations. The bias ratio is given by:

$$B = \frac{a+b}{a+c} \qquad (16)$$

A perfectly unbiased forecast method would predict the event the same amount of times the event occurred, resulting in a bias ratio of one. A bias ratio greater than one indicates the event was overforecast, a bias ratio less than one means the event was underforecast. Since the bias ratio doesn't take into account the number of times the "yes" forecast was actually correct, it is not a measure of accuracy (Wilks, 1995:241).

4.2.3 Forecast Skill.

Forecast skill scores measure the relative accuracy of a set of forecasts, based on a set of standard reference forecasts. Skill scores are expressed as a percentage improvement over the set of reference forecasts. Therefore, any skill score greater than zero shows improvement over the reference forecast technique, while a skill score less than zero indicates poorer skill. A skill score of zero indicates the proposed forecast technique is equal in skill to the reference technique. One popular measure of forecast skill for 2 x 2 contingency tables is the Hanssen-Kuipers discriminant.

4.2.3.1 Hanssen-Kuipers Discriminant or Kuipers Skill Score (KSS).

The KSS gives an "impartial and satisfactory" indication of forecast skill for scientific purposes (Bjornson, 1992:10). The reference forecast technique used in the Kuipers skill score is random forecasts, constrained to be unbiased. Therefore, the hypothetical random reference forecasts have a probability distribution equal to the climatology of the sample. Consequently, the probability of forecasting contrails equals the probability of

observing contrails, and the probability of not forecasting contrails equals the probability

of not observing contrails (Wilks, 1995:249).

4.2.3.2 Tests for Significance in 2 x 2 Contingency Tables.

For the statistical measures of accuracy, bias, and skill to be meaningful, it must

be shown that there is a connection or association between the column classification in a

contingency table (contrail observed) and the row classification (contrail forecast).

Otherwise, an apparently good relationship between observing contrails when they are

forecast (a large count for entry a in Figure 6) may be due entirely to chance (Kalbfleisch,

1979:148). In order to show such a relationship between the column and row

classifications (significance) exists, a test of independence must be performed.

Two events are independent if the probability of event B occurring, given that

event A has already occurred, is equal to the probability of event B occurring alone

(Devore, 1995:79). Applied to the contingency table shown in Figure 6, the probability

of observing a contrail, given that a contrail was forecast, equals the probability of

observing a contrail regardless of the forecast. To show there is an association between

the observations and the forecasts, we must reject the assumption of independence (show

dependence between column and row).

To show dependence in the contingency tables, a Fisher-Irwin exact test was

employed (due to the very small sample size of some of the tables) using a level of

significance of five percent (Sachs, 1984:370-372). If the p-value computed in the test

was less than 0.05, the notion of independence was rejected and the type of contrail

observed (yes/no) was declared dependent upon the forecast category. At a five percent

level of significance, there is only a 1 out of 20 probability that the forecast was correctly made by chance (Bjornson, 1992:10).

Contingency table significance is documented in the Results section of Chapter 5. Where the Fisher-Irwin test did not reject independence in the table (the association between columns and rows may be due to chance alone), caution must be exercised in interpreting the statistical results. Statistical insignificance or independence (at the five percent level) implies there is a greater than 1 in 20 probability that the results were obtained by chance. All figures and tables displaying results are accompanied by a statement of statistical significance.

5. Findings and Conclusions

5.1 Results

The statistical measures of accuracy, bias, and skill were applied to both sets of data as described in Chapter 3 (see Appendix E).

5.1.1 Edwards AFB Data.

Results of the statistical computations for the Edwards AFB data are shown in Tables 10 and 11. As the first row of each table shows, the Schrader and Hanson forecast methods were nearly equivalent when the data were considered as a whole (all flights). Since the two contingency tables generated by the 501 observations were shown to be significant by the Fisher-Irwin test, this result was probably not due to chance. However, analyzing the data as a whole does not reveal the flight-to-flight variability of atmospheric moisture conditions.

When computations were performed by flight, to test each method under varying relative humidity conditions, the Hanson algorithm's performance was found to be generally poor in a low relative humidity environment. However, due to a lack of balance in the contingency tables (most flights were conducted in conditions favorable to contrail formation), significance tests reveal this poor performance may be due to chance so these results are not conclusive.

5.1.1.1 Schrader Results.

The Schrader method was able to predict approximately three out of four contrails observed during the flight tests at Edwards AFB. In general, the Schrader algorithm was

able to detect 69.7 percent of all contrails and exhibited a low false alarm rate (20.7

percent). This method showed almost no bias (bias ratio of 1.011) but demonstrated only

a 19.2 percent increase in skill when compared to random forecasts. When the data were

broken out by flight, little variability in the statistics was apparent.

Table 10. Summary of Statistics for Edwards AFB Data (Schrader Method)

Flight Number	Sample Size	Hit Rate	Critical Success Index	False Alarm Rate	Bias Ratio	Kuipers Skill Score	Significance (P<0.05)
All Flights	501	0.697	0.663	0.207	1.011	0.192	Y
625	13	0.846	0.846	0.154	1.182	0	N
626	6	0.500	0.500	0.250	0.800	-0.400	N
627	2	1	1	0	1	0	N
628	14	0.286	0	0	0	0	N
629	7	0.857	0.857	0.143	1.167	0	N
630	2	1	1	0	1	0	N
632	28	0.429	0.273	0	0.273	0.273	N
633	36	0.722	0.688	0.214	1.077	0.246	N
635	20	0.750	0.750	0.250	1.333	0	N
636	18	0.444	0.231	0	0.231	0.231	N
637	20	0.850	0.833	0.167	1.200	0.400	Y
639	31	0.839	0.833	0.167	1.200	0.167	N
640	30	0.767	0.759	0.214	1.217	0.099	N
642	42	0.762	0.762	0.238	1.313	0	N
643	30	0.733	0.733	0.267	1.364	0	N
646	26	0.731	0.650	0.188	0.941	0.431	Y
648	21	0.762	0.762	0.238	1.313	0	N
649	44	0.705	0.690	0.275	1.29	0.089	N
652	20	0.800	0.733	0	0.733	0.733	N
653	21	0.619	0.556	0.231	0.867	0.167	N
655	26	0.615	0.545	0.200	0.789	0.203	N
656	26	0.577	0.522	0.333	1.059	0.039	N
660	18	0.778	0.714	0	0.714	0.714	Y

Table 11. Summary of Statistics for Edwards AFB Data (Hanson Method)

Flight Number	Sample Size	Avg RH (%)	Hit Rate	Critical Success Index	False Alarm Rate	Bias Ratio	Kuipers Skill Score	Significance (P<0.05)
All Flights	501	71	0.705	0.683	0.228	1.107	0.121	Y
625	13	94	0.846	0.846	0.154	1.182	0	N
626	6	25	0.167	0	0	0	0	N
627	2	52	1	1	0	1	0	N
628	14	47	0.429	0.333	0.333	0.600	-0.100	N
629	7	94	0.857	0.857	0.143	1.167	0	N
630	2	51	1	1	0	1	0	N
632	28	55	0.643	0.583	0.125	0.727	0.303	N
633	36	91	0.722	0.722	0.278	1.385	0	N
635	20	95	0.750	0.750	0.250	1.333	0	N
636	18	31	0.278	0	0	0	0	N
637	20	54	0.800	0.778	0.176	1.133	0.333	N
639	31	52	0.774	0.750	0.125	0.960	0.340	N
640	30	79	0.767	0.767	0.233	1.304	0	N
642	42	74	0.762	0.762	0.238	1.313	0	N
643	30	84	0.733	0.733	0.267	1.364	0	N
646	26	65	0.692	0.667	0.304	1.353	0.163	N
648	21	99	0.762	0.762	0.238	1.313	0	N
649	44	87	0.705	0.705	0.295	1.419	0	N
652	20	54	0.800	0.733	0	0.733	0.733	N
653	21	76	0.714	0.700	0.263	1.267	0.100	N
655	26	64	0.692	0.667	0.238	1.105	0.128	N
656	26	66	0.615	0.565	0.316	1.118	0.098	N
660	18	31	0.778	0.714	0	0.714	0.714	Y

5.1.1.2 Hanson Results

As noted, the Hanson method performed as well as the Schrader algorithm when all flights were analyzed as a whole. Overall, the Hanson forecasts were able to detect 70.5 percent of the observed contrails, exhibited a 22.8 percent false alarm rate, showed very little bias (bias ratio 1.107), and demonstrated a 12.1 percent increase in skill over using random forecasts. However, as stated before, the Hanson method tended to show a

marked decrease in performance when flights with low average relative humidity were examined (although Fisher-Irwin tests indicate this may be due to chance alone).

A plot of the Hanson versus Schrader hit rate is shown in Figure 8. In the figure, each average relative humidity value from Table 11 (which represents a specific flight) is plotted at the intersection of the hit rates for the two forecast methods.
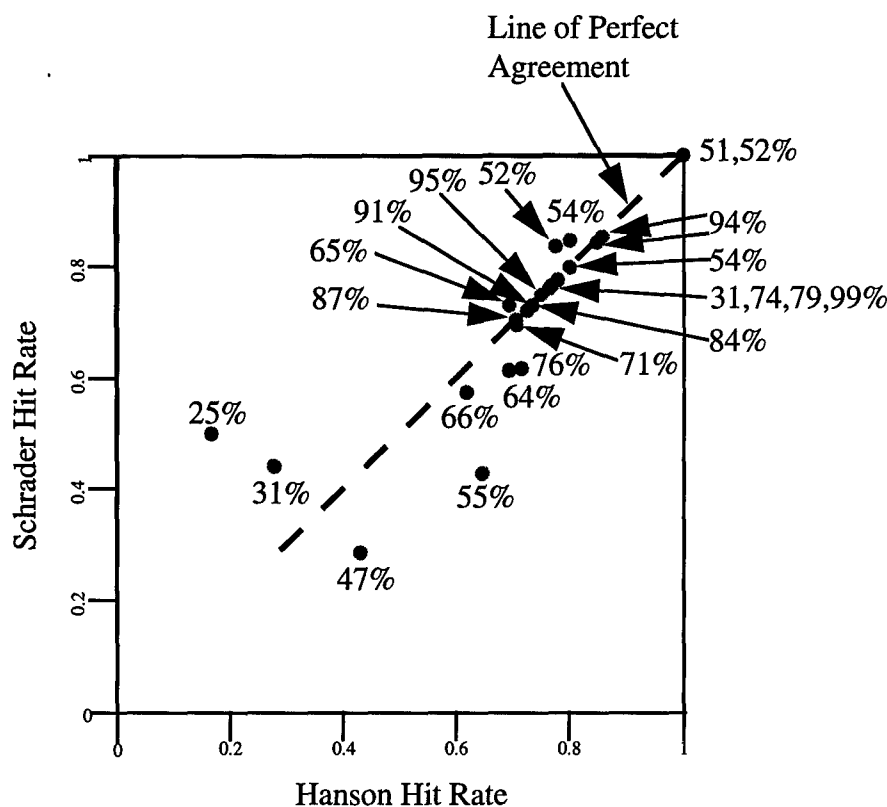
Figure 8. Hanson vs. Schrader Hit Rate as a Function of Relative Humidity (Edwards AFB Data)

If both methods produce the same hit rate for the same flight (relative humidity), the point will lie on a 45 degree diagonal (the line of perfect agreement). As shown in

Figure 8, the Hanson and Schrader methods appear to agree more closely under conditions of high relative humidity. Some smaller relative humidity values also lie close to the line, but this is probably due to small sample size variations. In general, the lowest relative humidity values lie above and to the left of the line of perfect agreement, showing the Schrader method performs better under these (drier) conditions. Again, due to the lack of significance as a result of generally favorable contrail conditions, these results are not conclusive.

Bar graphs, showing statistics for the two methods by flight number, again infer the Hanson method's lack of skill when the ambient relative humidity is low. As shown in Figures 9 through 12, the two algorithms produce nearly identical results under moist atmospheric conditions. However, as stated earlier, caution must be exercised in interpreting these results since all but the cumulative contingency tables proved to be independent.
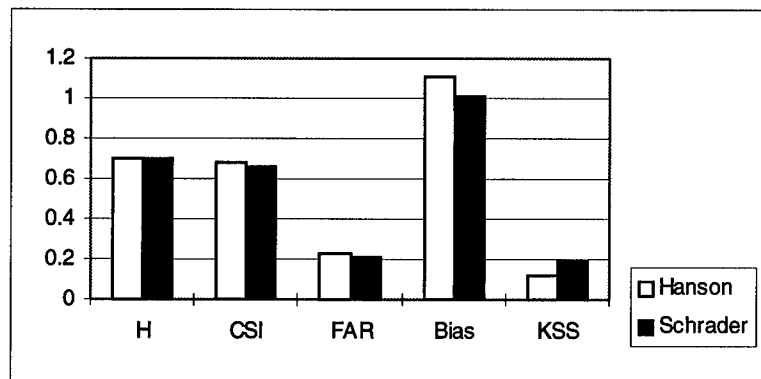
Figure 9. Edwards AFB Statistics, All Flights (Avg RH=71%, n=501, Dependent)
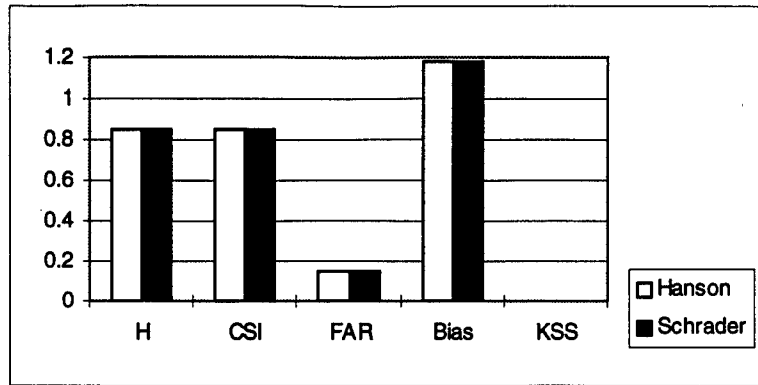
Figure 10. Edwards AFB Statistics, Flight 625 (Avg RH=94%, n=13, Independent)
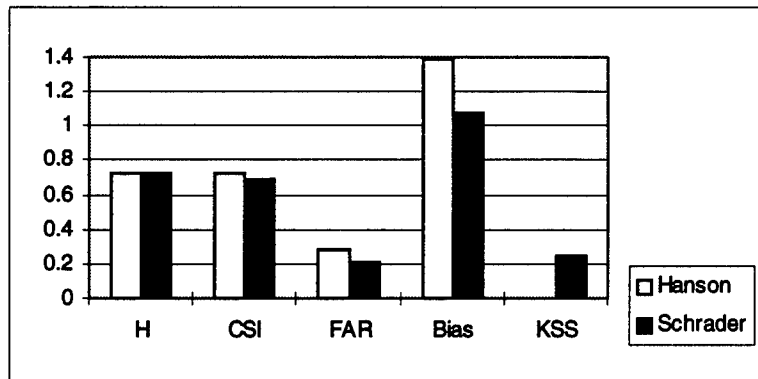
Figure 11. Edwards AFB Statistics, Flight 633 (Avg RH=91%, n=36, Independent)
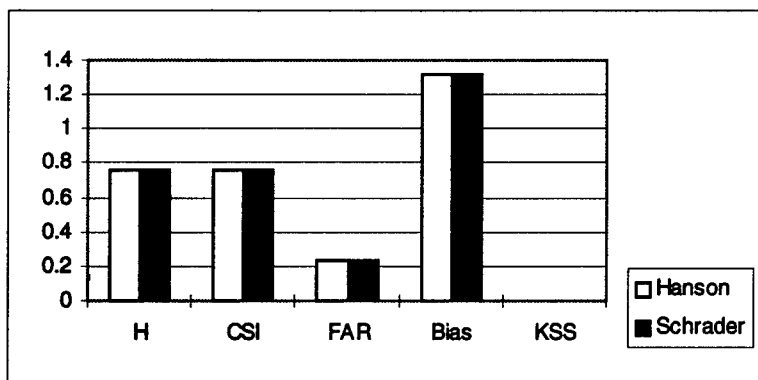
Figure 12. Edwards AFB Statistics, Flight 648 (Avg RH=99%, n=21, Independent)

However, on flights when the relative humidity was low, the Hanson method's

performance was greatly reduced as shown in Figures 13 and 14.
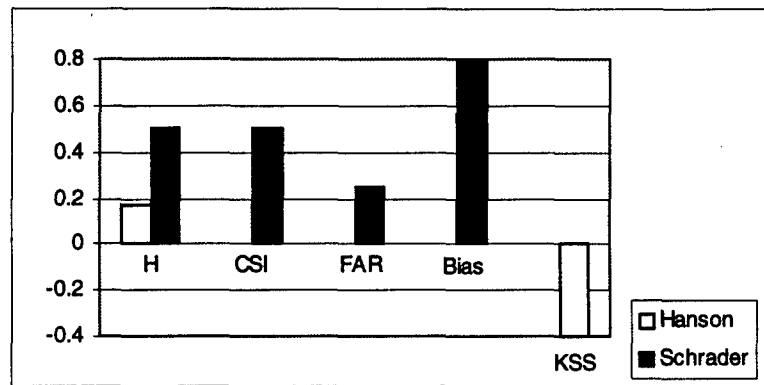
Figure 13. Edwards AFB Statistics, Flight 626 (Avg RH=25%, n=6, Independent)
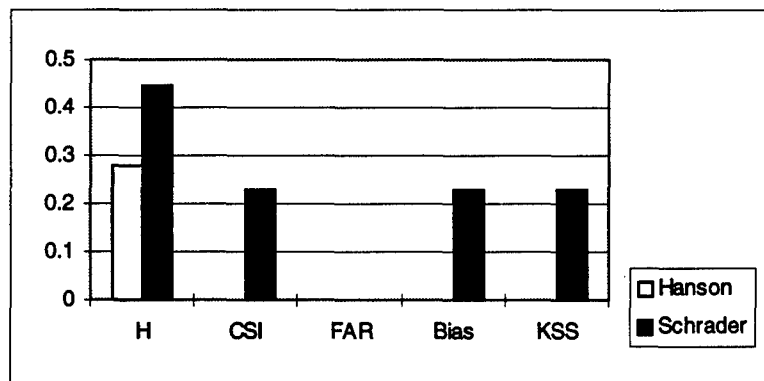
Figure 14. Edwards AFB Statistics, Flight 636 (Avg RH=31%, n=18, Independent)

Since the Edwards AFB data were collected under persistently "unique weather

conditions" of high ambient relative humidity (Saatzer, 1995: ix), environmental factors

were more favorable to contrail formation than not. As a result, the Fisher-Irwin tests of

significance conclusively show only that the Hanson and Schrader forecast methods are

equivalent under moist atmospheric conditions. Any conclusions drawn about the poor performance of the Hanson algorithm under dry conditions are suspect due to small sample size limitations.

5.1.2 WPAFB Data.

Statistical results for the WPAFB data are shown in Tables 12-14. As the first row of each table shows, the three forecast methods performed equally well using the 40/70/10 percent relative humidity assumption. However, when actual relative humidity measurements were used, the Hanson method's performance decreased sharply. Since all methods' contingency tables proved to be significant by the Fisher-Irwin test (when all 98 observations were analyzed as a whole), this result is deemed conclusive. On this basis, the data were further analyzed by relative humidity category ("moist" or "dry"), day, and engine type. All calculations on subsets of the data were performed with actual relative humidity values, in an attempt to determine where the Hanson algorithm failed to produce satisfactory results.

5.1.2.1 Schumann Results.

The Schumann method performed reasonably well on all days using the 40/70/10 percent relative humidity assumption (see Table 12). This algorithm was able to detect 77.6 percent of the observed contrails, and exhibited a fairly low false alarm rate (14.7 percent). Since the bias ratio was one, it was not prone to over- or under-forecasting contrails and showed a 37.5 percent increase in skill compared to using random forecasts. Using ambient relative humidity measurements for all days offered a significant increase in skill (48.2 percent) while other parameters changed little. The Schumann algorithm

also produced good results and showed little variability about the mean (all days) using

the day-to-day observations.

Table 12. Summary of Statistics for WPAFB Data (Schumann Method)

Date or Type	Sample Size	Hit Rate	Critical Success Index	False Alarm Rate	Bias Ratio	Kuipers Skill Score	Significance (P<0.05)
All Days (Assumed RH)	98	0.776	0.744	0.147	1.000	0.375	Y
All Days (Ambient RH)	98	0.765	0.720	0.106	0.880	0.482	Y
"Moist" Days (Avg RH ≥20%)	33	0.788	0.788	0.071	0.903	-0.161	N
"Dry" Days (Avg RH <20%)	65	0.754	0.673	0.132	0.864	0.512	Y
11 Sep 96	4	0.500	0	0	0	0	N
19 Sep 96	9	0.778	0.778	0.125	1.000	-0.125	N
30 Sep 96	6	0.667	0.667	0	0.667	0	N
2 Oct 96	6	1.000	1.000	0	1.000	1.000	N
3 Oct 96	9	1.000	1.000	0	1.000	1.000	Y
4 Oct 96	29	0.793	0.793	0.042	0.857	-0.179	N
5 Oct 96	4	0.750	0.750	0.250	1.333	0	N
7 Oct 96	10	0.625	0.500	0.500	2.000	0.400	N
8 Oct 96	3	0.667	0	0	0	0	N
11 Oct 96	8	0.714	0.667	0.200	1.000	0.300	N
16 Oct 96	6	0.667	0.500	0	0.500	0.500	N
17 Oct 96	9	0.778	0.714	0	0.714	0.714	N
Low Bypass	28	0.714	0.556	0.091	0.647	0.497	Y
High Bypass	70	0.786	0.766	0.109	0.948	0.345	Y

5.1.2.2 Schrader Results.

Tables 12 and 13 illustrate that the Schumann and Schrader forecast methods are

statistically analogous, exhibiting the same hit rate and nearly equal levels of skill.

However, this result was expected because both algorithms produced very similar critical

temperatures (see Appendix B). Overall, like Schumann's algorithm, the Schrader

method performed well under all relative humidity conditions.

Table 13. Summary of Statistics for WPAFB Data (Schrader Method)

Date or Type	Sample Size	Hit Rate	Critical Success Index	False Alarm Rate	Bias Ratio	Kuipers Skill Score	Significance (P<0.05)
All Days (Assumed RH)	98	0.776	0.741	0.137	0.973	0.405	Y
All Days (Ambient RH)	98	0.755	0.707	0.108	0.867	0.469	Y
"Moist" Days (Avg RH ≥20%)	33	0.788	0.788	0.071	0.903	-0.161	N
"Dry" Days (Avg RH <20%)	65	0.738	0.653	0.135	0.841	0.489	Y
11 Sep 96	4	0.500	0	0	0	0	N
19 Sep 96	9	0.778	0.778	0.125	1.000	-0.125	N
30 Sep 96	6	0.667	0.667	0	0.667	0	N
2 Oct 96	6	1.000	1.000	0	1.000	1.000	N
3 Oct 96	9	1.000	1.000	0	1.000	1.000	Y
4 Oct 96	29	0.793	0.793	0.042	0.857	-0.179	N
5 Oct 96	4	0.750	0.750	0.250	1.333	0	N
7 Oct 96	10	0.625	0.500	0.500	2	0.400	N
8 Oct 96	3	0.667	0	0	0	0	N
11 Oct 96	8	0.714	0.667	0.200	1.000	0.300	N
16 Oct 96	6	0.500	0.250	0	0.250	0.250	N
17 Oct 96	9	0.778	0.714	0	0.714	0.714	N
Low Bypass	28	0.679	0.500	0.100	0.588	0.439	Y
High Bypass	70	0.786	0.766	0.109	0.948	0.345	Y

5.1.2.3 Hanson Results.

The Hanson method performed as well as the others using the assumed (40/70/10

percent) relative humidity assumption. However, when the actual relative humidity was

used, the performance of the algorithm was reduced by nearly 50 percent (see Table 14).

The only difference in the data, between the first two rows of each table, is the relative humidity measurement method.

Table 14. Summary of Statistics for WPAFB Data (Hanson Method)

Date or Type	Sample Size	Avg RH (%)	Hit Rate	Critical Success Index	False Alarm Rate	Bias Ratio	Kuipers Skill Score	Significance (P<0.05)
All Days (Assumed RH)	98	38	0.755	0.707	0.108	0.867	0.469	Y
All Days (Ambient RH)	98	12	0.469	0.325	0.074	0.360	0.246	Y
"Moist" Days (Avg RH ≥20%)	33	28	0.758	0.758	0.074	0.871	-0.194	N
"Dry" Days (Avg RH <20%)	65	9	.323	0	0	0	0	N
11 Sep 96	4	8	0.500	0	0	0	0	N
19 Sep 96	9	5	0.111	0	0	0	0	N
30 Sep 96	6	8	0	0	0	0	0	N
2 Oct 96	6	8	0.250	0	0	0	0	N
3 Oct 96	9	12	0.444	0	0	0	0	N
4 Oct 96	29	31	0.793	0.793	0.042	0.857	-0.179	N
5 Oct 96	4	25	0.500	0.500	0.333	1.000	-0.333	N
7 Oct 96	10	10	0.625	0	0	0	0	N
8 Oct 96	3	6	0.667	0	0	0	0	N
11 Oct 96	8	16	0.286	0	0	0	0	N
16 Oct 96	6	9	0.333	0	0	0	0	N
17 Oct 96	9	8	0.222	0	0	0	0	N
Low Bypass	28	22	0.607	0.353	0	0.353	0.353	N
High Bypass	70	17	0.414	0.317	0.095	0.362	0.161	N

Using the 40/70/10 percent assumption, the average relative humidity for all days was 38 percent (see Table 8). Using the radiosonde (actual) data, the average relative humidity for all days was only 12 percent. Therefore, using the 40/70/10 percent relative humidity assumption greatly overestimated the actual moisture profile. Since the critical

temperatures for contrail formation from the Hanson method are in good agreement with the other methods at high relative humidity (see Appendix B), similar results for all three methods are expected under moist conditions. However, under drier conditions, the Hanson algorithm's performance diminishes. Therefore, statistics were calculated on a moisture category and daily basis to explore the Hanson method's dependence on relative humidity.

A plot of the Hanson versus Schrader hit rate, like Figure 8 except for the WPAFB data, is shown in Figure 15. It shows the same general tendency for agreement under higher relative humidity conditions as before. However, as noted with the Edwards AFB data, almost all of the daily contingency tables showed independence of contrail observations and forecasts, making any inferences drawn from this diagram suspect (see Table 14).
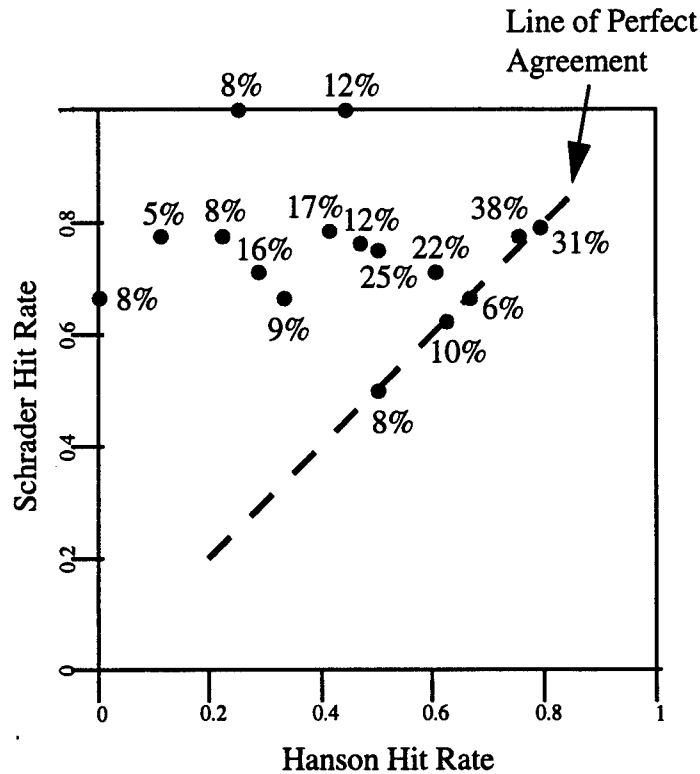
Figure 15. Hanson vs. Schrader Hit Rate as a Function of Relative Humidity (WPAFB Data)

Bar graphs, showing statistics for the three methods under varying relative humidity conditions, further imply the Hanson method's lack of skill when the relative humidity is low. As shown in Figure 16, the algorithms produced nearly identical results under the 40/70/10 percent relative humidity assumption. However, when the actual ambient relative humidity was used, the Hanson method's performance dropped markedly as shown in Figure 17.
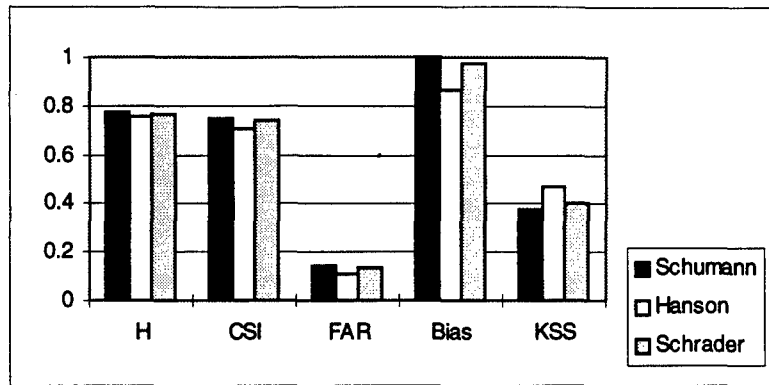
Figure 16. WPAFB Statistics, All Days (Assumed Avg RH=38%, n=98, Dependent)
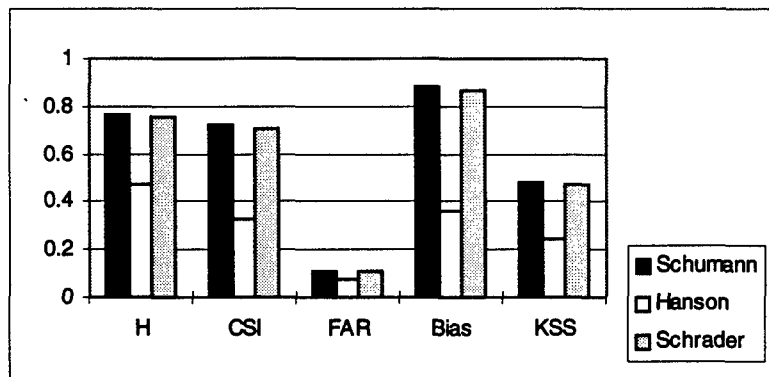
Figure 17. WPAFB Statistics, All Days (Ambient Avg RH=12%, n=98, Dependent)

In order to further demonstrate the Hanson method's lack of skill under dry

conditions, and to maintain a relatively large sample size, the database was divided into

two categories based on the in-situ relative humidity. Those days with an average relative

humidity of greater than or equal to 20 percent were characterized as "moist", while those

with lower values were designated "dry."

As shown in Tables 12-14, all methods were roughly equivalent when the

observations were taken under "moist" conditions. Since each algorithm tends to forecast

contrails frequently in a "moist" environment, Fisher-Irwin tests revealed the contingency

tables generated from this data were independent (the results may be due to chance).

However, when the "dry" days were analyzed, the Hanson algorithm's utility decreased,

while the other two methods showed a marked increase in skill score (see Figures 18-19).
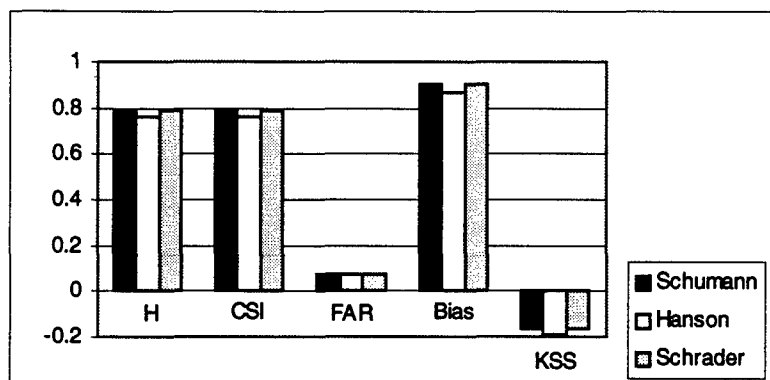
Figure 18. WPAFB Statistics, "Moist" Days (Avg RH=28%, n=33, Independent)
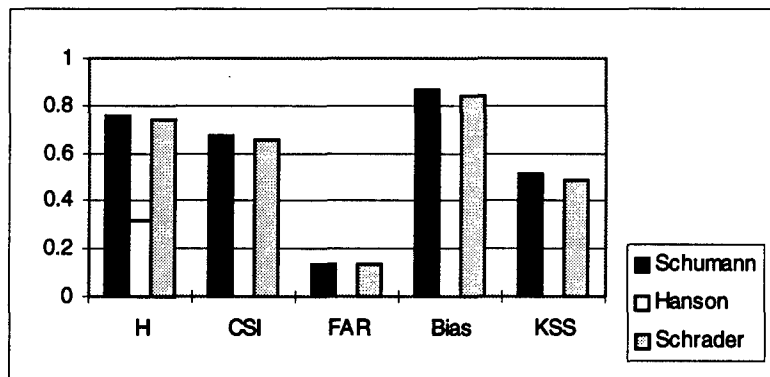
Figure 19. WPAFB Statistics, "Dry" Days (Avg RH=9%, n=65, Hanson Independent)

Although the sample sizes become quite small, analyzing the data on a daily basis

further illustrates each method's performance under varying atmospheric conditions.

Figures 20-24 confirm the trend evident in the "moist/dry" categorization (the tendency

for the Hanson method to perform poorly under low relative humidity conditions), given

that these results are independent and may be due to chance.
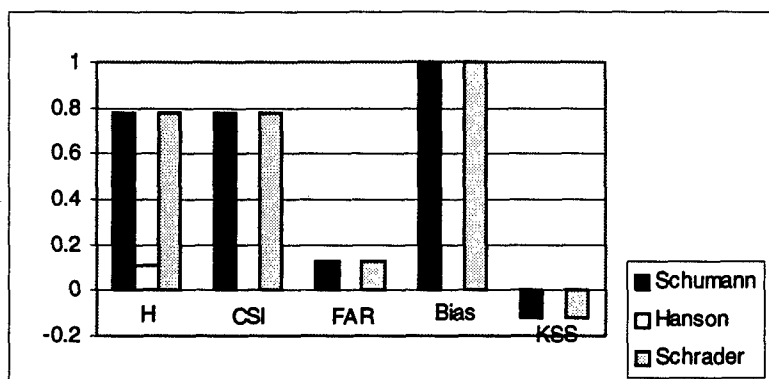
Figure 20. WPAFB Statistics, 19 Sep 96 (Avg RH=5%, n=9, Independent)
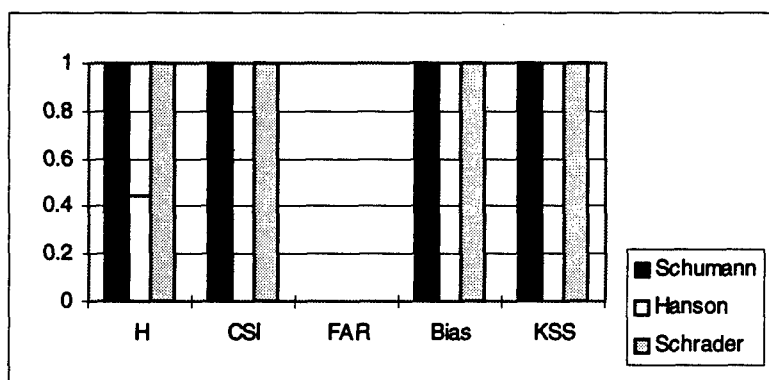
Figure 21. WPAFB Statistics, 3 Oct 96 (Avg RH=12%, n=9, Hanson Independent)
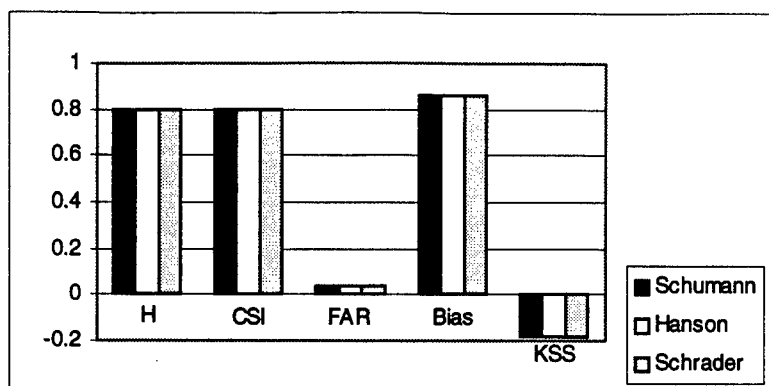
Figure 22. WPAFB Statistics, 4 Oct 96 (Avg RH=31%, n=29, Independent)
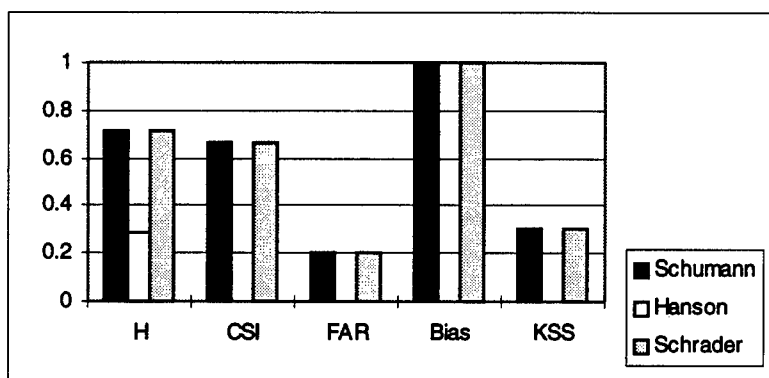
Figure 23. WPAFB Statistics, 11 Oct 96 (Avg RH=16%, n=8, Independent)
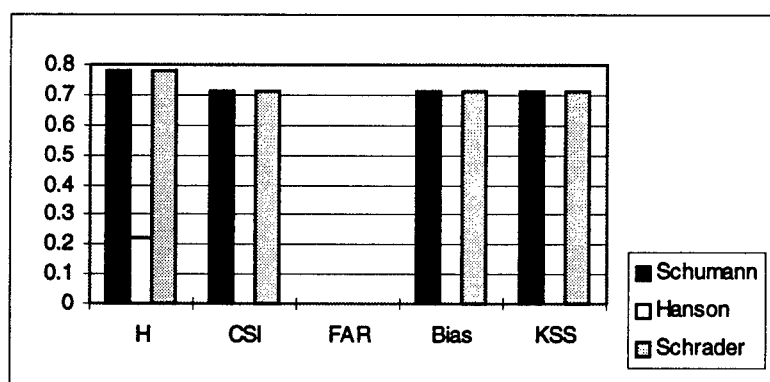
Figure 24. WPAFB Statistics, 17 Oct 96 (Avg RH=8%, n=9, Independent)

Figures 25 and 26 show each algorithm's performance when observations are broken out by aircraft type (low or high bypass engines). Surprisingly, due to the colder temperatures required for contrail formation by the Hanson algorithm, Hanson appears to perform better when used for low bypass aircraft. However, this may be coincidental since the low bypass aircraft generally flew at lower altitudes (average pressure altitude of 250mb as compared to 225mb for high bypass aircraft) and thus would generally fly in conditions of higher relative humidity. In addition, both Hanson contingency tables could not be declared dependent and variations may be due to chance.

A comparison of theoretical critical temperatures for each method illustrates why the Hanson algorithm performs poorly under dry conditions. Assuming a high bypass contrail factor, "average" critical temperatures were computed for all observations and for each day (see Table 8).
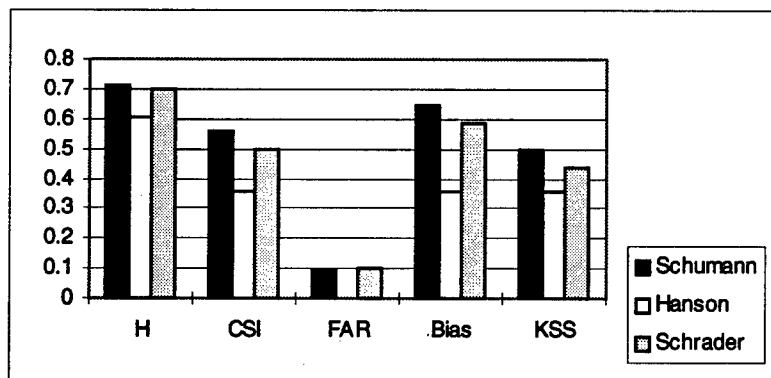
Figure 25. WPAFB Statistics, Low Bypass Engines Only (Avg RH=22%, n=28, Hanson Independent)
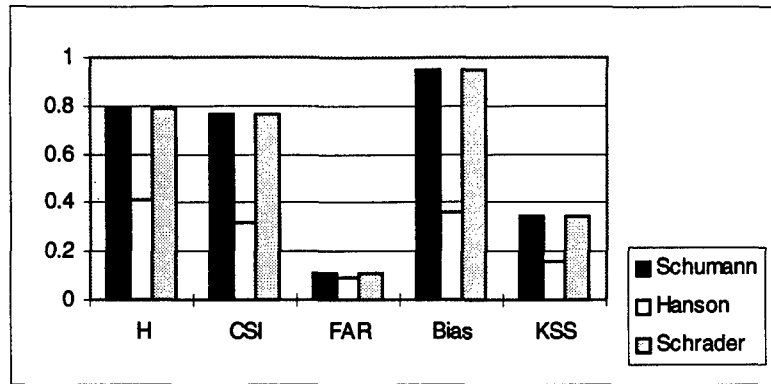
Figure 26. WPAFB Statistics, High Bypass Engines Only (Avg RH=17%, n=70, Hanson Independent)

These calculations are illustrated in Table 15. As shown in the table, the theoretical critical temperatures for the Schumann and Schrader methods differ by less than one degree Celsius under all circumstances. Thus, they produce statistically equivalent results. However, the Hanson method predicts much colder temperatures for contrail formation, especially when the ambient relative humidity is low. In fact, the Hanson critical temperature is 10 or more degrees colder than either of the other two methods on most days. Therefore, as suggested by the statistics above, the critical temperatures predicted by the Hanson algorithm are simply too cold to adequately forecast contrails under dry conditions.

Table 15. Average Critical Temperatures for WPAFB Data

Date or Type	Average Flight Level (mb)	Average Ambient RH (%RH)	Average Ambient Temp (°C)	Schumann Critical Temp (°C)	Schrader Critical Temp (°C)	Hanson Critical Temp (°C)
All Days	232	12	-52.1	-51.7	-52.1	-62.8
11 Sep 96	230	8	-49.0	-51.8	-52.3	-66.1
19 Sep 96	204	5	-50.9	-52.9	-53.5	-70.7
30 Sep 96	231	8	-51.6	-51.7	-52.2	-66.1
2 Oct 96	213	8	-52.0	-52.5	-53.0	-66.7
3 Oct 96	247	12	-55.3	-51.1	-51.5	-62.23
4 Oct 96	234	31	-56.3	-51.1	-51.2	-54.4
5 Oct 96	217	25	-54.8	-52.0	-52.2	-57.0
7 Oct 96	239	10	-52.4	-51.4	-51.9	-64.0
8 Oct 96	247	6	-47.3	-51.1	-51.7	-67.8
11 Oct 96	236	16	-52.5	-51.5	-51.8	-60.2
16 Oct 96	250	9	-51.0	-51.0	-51.5	-64.5
17 Oct 96	229	8	-51.6	-51.8	-52.3	-66.2

5.2 Conclusions

There is evidence to suggest the Hanson forecast method fails to improve on existing techniques to predict contrails under low ambient relative humidity conditions, as claimed. However, under moist conditions, the Hanson algorithm is nearly identical to the Schumann and Schrader methods, as should be the case by comparing the standard critical temperatures under moist conditions (see Appendix B). Since the Hanson method fails to adequately predict contrails under all environmental conditions, it is not recommended for operational forecasting.

As a secondary conclusion, it was noted that the Schumann and Schrader contrail forecast algorithms showed statistically equal performance under all atmospheric conditions. Even though they were derived in a different manner, both methods appear to

detect roughly 70 to 75 percent of all observed contrails and demonstrate comparable levels of forecast skill. Both methods also showed a slight increase in skill when used to predict contrails in a dry environment.

5.3 Recommendations for Further Research

Additional WPAFB data should be collected and the algorithms tested with a larger dataset. Although 98 observations are adequate when the data are taken as a whole, the analysis of individual days with the current data results in prohibitively small sample sizes. Since a statistically significant sample of the "yes" and "no" forecast populations is difficult to obtain with so few day-to-day observations, it is difficult to draw valid conclusions on a day-to-day (or atmospheric profile) basis.

The small daily sample sizes were mainly a result of the time of day most observations were made (approximately 1400 LT). It was noted that most high altitude air traffic in the Dayton area occurs during the early morning hours (approximately 0730 to 0900 LT). On the one day contrails were observed at this time, 29 aircraft were positively identified. Therefore, data should be collected during the peak traffic hours to increase the likelihood of obtaining large sample sizes.

Additionally, observations should be made on "borderline" contrail days if possible (days when contrails are just as likely to form as not). Observing contrails only during conditions strongly favorable (or unfavorable) for their development tends to skew the data. This is the primary reason why most daily (or flight) contingency tables could not be declared independent. By not having a representative population of observations from the "no" forecast category, not enough information was available to conclusively

73

state that the observations were associated with the forecasts (D. Reynolds, 1997, personal communication).

It is also recommended that the Schumann and Schrader algorithms be investigated further on a day-to-day basis using larger sample sizes. This may provide evidence as to why they only detect 70 to 75 percent of observed contrails. Investigating those days when each method's performance suffered may indicate the need for the application of an empirical correction to the critical temperature (based upon either the atmospheric lapse rate, stability, or some other atmospheric parameter).

Finally, it is recommended that the Coleman contrail forecast technique (Coleman, 1996:2270), published while this thesis was in draft form, be tested to determine whether it outperforms the method currently in use at AFGWC.

Appendix A: Corrections to Papers

The Hanson and Schrader papers contain typographical errors which make it impossible to reproduce the critical temperatures given in the appendices. This appendix shows the correct equations so they may be used by the reader. In the Hanson paper, Equations (2) and (4) should be changed to (Hanson, 1995:2401):

$$\log_{10}(e_w) = 23.832241 - 5.02808 \cdot \log_{10} \cdot (T) - 1.3816 \cdot 10^{-7} \cdot \left[10^{(11.334 - 0.0303998 \cdot (T))}\right]$$

$$+ 8.1328 \cdot 10^{-3} \cdot \left[10^{\left(3.49149 - \frac{1302.8844}{T}\right)}\right] - \frac{2949.076}{T}$$

$$P_8 = 10.5961 \cdot \frac{10^{\left(3.49149 - \frac{1302.8844}{T}\right)}}{T^2} \cdot \ln(10)$$

In Equation (3) of the Schrader paper (Schrader, 1994:6), all log(n) operators should be changed to ln(n).

Appendix B: Critical Temperatures for Contrail Formation

Critical temperatures were computed for each algorithm, assuming a high bypass engine, using the program at Appendix E. Theoretical critical temperatures for the Schumann method are shown in Table B1.

Table B1. Schumann Critical Temperatures (Propulsion Efficiency: 0.308)

Pressure (mb)	Critical Temp RH=0% (°C)	Critical Temp RH=10% (°C)	Critical Temp RH=40% (°C)	Critical Temp RH=70% (°C)	Critical Temp RH=100% (°C)
50	-65.3	-65.3	-64.5	-62.6	-57.1
100	-59.4	-59.4	-58.6	-56.6	-50.7
200	-53.2	-53.1	-52.3	-50.1	-43.9
300	-49.3	-49.3	-48.4	-46.1	-39.7
400	-46.5	-46.5	-45.5	-43.2	-36.5
500	-44.2	-44.2	-43.2	-40.9	-34.0
600	-42.4	-42.3	-41.3	-38.9	-32.0
700	-40.7	-40.7	-39.7	-37.2	-30.2
800	-39.3	-39.3	-38.3	-35.8	-28.6
1000	-36.9	-36.8	-35.8	-33.2	-25.9

Critical temperatures for the Schrader method are shown in Table B2. Slight differences between these values, and those printed in the Schrader paper (Schrader, 1994:14) are probably due to the secant method that MATHCAD uses to solve Equation (12) in Chapter III. Table B3 shows the maximum difference between the MATHCAD solution and the critical temperatures as given in the paper (for flight levels equal to or above 300mb).

Table B2. Schrader Critical Temperatures (Contrail Factor: $0.039\text{gkg}^{-1}\text{K}^{-1}$)

Pressure (mb)	Critical Temp RH=0% (°C)	Critical Temp RH=10% (°C)	Critical Temp RH=40% (°C)	Critical Temp RH=70% (°C)	Critical Temp RH=100% (°C)
50	-65.8	-65.5	-64.4	-62.9	-57.7
100	-60.0	-59.7	-58.6	-56.9	-51.4
200	-53.8	-53.5	-52.3	-50.5	-44.6
300	-50.0	-49.7	-48.4	-46.6	-40.4
400	-47.2	-46.9	-45.6	-43.6	-37.3
500	-45.0	-44.6	-43.3	-41.3	-34.9
600	-43.1	-42.8	-41.4	-39.4	-32.8
700	-41.5	-41.2	-39.8	-37.7	-31.0
800	-40.1	-39.7	-38.3	-36.3	-29.5
1000	-37.7	-37.3	-35.9	-33.8	-26.8

Table B3. Difference Between MATHCAD and Paper Critical Temperatures for Flight Levels Equal to or Above 300 mb (Schrader Method)

Relative Humidity (%)	Maximum Temp Difference (°C)
0	MATHCAD 0.005 too warm
10	MATHCAD 0.006 too warm
40	MATHCAD 0.220 too warm
70	MATHCAD 1.038 too warm
100	MATHCAD 0.081 too cold

Slightly greater temperature differences exist at flight levels below 300mb (at higher pressures), but these do not affect the calculations in this thesis since all contrail data were gathered above these altitudes.

Critical temperatures for the Hanson method are shown in Table B4. Note the lowest relative humidity value for which critical temperatures can be calculated is one percent. The maximum difference between the MATHCAD solution and the published

values, equal to or above 300mb, for all relative humidity conditions is 0.03°C

(MATHCAD computed value) too cold (Hanson, 1995:2404).

Table B4. Hanson Critical Temperatures (Contrail Factor: $0.039 gkg^{-1}K^{-1}$)

Pressure (mb)	Critical Temp RH=1% (°C)	Critical Temp RH=10% (°C)	Critical Temp RH=40% (°C)	Critical Temp RH=70% (°C)	Critical Temp RH=100% (°C)
50	-90.7	-75.9	-65.5	-60.8	-57.7
100	-86.6	-70.9	-59.7	-54.7	-51.4
200	-82.2	-65.5	-53.5	-48.2	-44.6
300	-79.5	-62.1	-49.7	-44.1	-40.4
400	-77.5	-59.7	-46.9	-41.2	-37.4
500	-75.9	-57.7	-44.6	-38.8	-34.9
600	-74.6	-56.1	-42.8	-36.8	-32.8
700	-73.5	-54.7	-41.2	-35.1	-31.0
800	-72.5	-53.5	-39.8	-33.6	-29.5
1000	-70.9	-51.4	-37.4	-31.0	-26.8

Table C1. Wright-Patterson AFB Data

Date	Aircraft Type	Contrail Factor (g/kg-°C)	Contrail	Flight Level (kft)	Pressure (mb)	Ambient Temp (°C)	RH (In Situ)	RH (40/70/10)
11/Sep	DC9	0.034	N	330	262	-47	12	40
11/Sep	757	0.039	Y	410	178.6	-53.9	2	40
11/Sep	LEAR35	0.039*	Y	370	216.3	-49.3	7	40
11/Sep	DC9	0.034	N	330	261.6	-46.5	12	40
19/Sep	F16	0.034	Y	410	178.6	-58.6	5	40
19/Sep	737	0.039*	Y	350	238	-49.2	7	40
19/Sep	CL60	0.039*	Y	410	178.6	-58.6	5	40
19/Sep	777	0.039	Y	370	216.3	-53.3	7	40
19/Sep	747	0.039	Y	370	216.3	-53.3	7	40
19/Sep	747	0.039	Y	370	216.3	-53.3	7	40
19/Sep	C650	0.039*	Y	390	196.5	-56.5	7	40
19/Sep	G2	0.039*	Y	390	196.5	-56.5	7	40
19/Sep	757	0.039	N	390	196.5	-56.5	7	40
30/Sep	MD80	0.034	Y	330	261.6	-45.4	8	40
30/Sep	MD80	0.034	Y	370	216.3	-54.2	6	40
30/Sep	757	0.039	Y	330	261.6	-45.4	8	40
30/Sep	747	0.039	Y	370	216.3	-54.2	6	40
30/Sep	767	0.039	Y	370	216.3	-54.2	6	40
30/Sep	CL60	0.039*	Y	370	216.3	-54.2	6	40
02/Oct	C501	0.039*	Y	390	196.5	-56.9	4	40
02/Oct	N265	0.039*	Y	390	196.5	-56.9	4	40
02/Oct	757	0.039	Y	390	196.5	-56.9	4	40
02/Oct	DC9	0.034	N	330	261.6	-47.3	11	40
03/Oct	MD80	0.034	N	310	287	-44.7	11	40
03/Oct	757	0.039	Y	350	238	-54.7	11	40
03/Oct	737	0.039*	N	330	261.6	-49.9	12	40
03/Oct	757	0.039	Y	390	196.5	-61	12	40
03/Oct	757	0.039	Y	370	216.3	-58.4	12	40
03/Oct	767	0.039	Y	350	238	-54.7	11	40
03/Oct	737	0.039*	N	310	287	-44.7	11	40
03/Oct	757	0.039	Y	350	238	-54.7	11	40
03/Oct	DC9	0.034	N	330	261.6	-49.9	12	40
04/Oct	757	0.039	Y	350	238	-54.6	35	40
04/Oct	N265	0.039*	Y	390	196.5	-63.7	27	40
04/Oct	737	0.039*	N	350	238	-54.6	35	40
04/Oct	757	0.039	Y	310	287	-44.2	31	40
04/Oct	AIRBUS320	0.039	Y	350	238	-54.6	35	40
04/Oct	757	0.039	Y	390	196.5	-63.7	27	40
04/Oct	767	0.039	Y	350	238	-54.6	35	40
04/Oct	747	0.039	Y	330	261.6	-49.4	37	40
04/Oct	767	0.039	Y	350	238	-54.6	35	40

Date	Aircraft Type	Contrail Factor (g/kg-°C)	Contrail	Flight Level (kft)	Pressure (mb)	Ambient Temp (°C)	RH (In Situ)	RH (40/70/10)
04/Oct	747	0.039	Y	350	238	-54.6	35	40
04/Oct	767	0.039	Y	370	216.3	-60	30	40
04/Oct	767	0.039	Y	350	238	-54.6	35	40
04/Oct	MD88	0.034	Y	350	238	-54.6	35	40
04/Oct	757	0.039	Y	350	238	-54.6	35	40
04/Oct	727	0.034	Y	330	261.6	-49.4	37	40
04/Oct	LEAR35	0.039*	Y	370	216.3	-60	30	40
04/Oct	767	0.039	Y	350	238	-54.6	35	40
04/Oct	727	0.034	Y	370	216.3	-60	30	40
04/Oct	DC9	0.034	Y	330	261.6	-49.4	37	40
04/Oct	727	0.034	Y	330	261.6	-49.4	37	40
04/Oct	747	0.039	Y	390	196.5	-63.7	27	40
04/Oct	757	0.039	Y	370	216.3	-60	30	40
04/Oct	AIRBUS320	0.039	Y	370	216.3	-60	30	40
04/Oct	DC9	0.034	Y	350	238	-54.6	35	40
04/Oct	L1011	0.039	Y	350	238	-54.6	35	40
04/Oct	DC9	0.034	Y	350	238	-54.6	35	40
04/Oct	MD80	0.034	Y	350	238	-54.6	35	40
04/Oct	757	0.039	Y	370	216.3	-60	30	40
04/Oct	727	0.034	Y	350	238	-54.6	35	40
05/Oct	737	0.039*	N	370	216.3	-59	23	40
05/Oct	737	0.039*	Y	370	216.3	-59	23	40
05/Oct	LEAR35	0.039*	Y	390	196.5	-61.4	22	70
05/Oct	737	0.039*	Y	350	238	-53.9	25	40
07/Oct	DC9	0.034	N	350	238	-53.9	25	40
07/Oct	737	0.039*	N	350	238	-53.9	25	40
07/Oct	727	0.034	Y	370	216.3	-55.6	10	40
07/Oct	AIRBUS320	0.039	N	350	238	-51.6	11	40
07/Oct	CL65	0.039*	Y	370	216.3	-55.6	10	40
07/Oct	757	0.039	Y	370	216.3	-55.6	10	40
07/Oct	KC135R	0.039	N	310	287	-42.9	12	40
07/Oct	727	0.034	N	330	261.6	-47.7	12	40
08/Oct	727	0.034	Y	310	287	-45.3	30	70
08/Oct	AIRBUS320	0.039	N	350	238	-45.3	1	10
08/Oct	757	0.039	N	370	216.3	-47.6	1	10
11/Oct	767	0.039	Y	350	238	-54.3	20	40
11/Oct	AIRBUS320	0.039	N	350	238	-54.3	20	40
11/Oct	DC9	0.034	N	330	261.6	-50.5	28	40
11/Oct	757	0.039	Y	370	216.3	-55.4	14	70
11/Oct	757	0.039	Y	350	238	-54.3	20	40
11/Oct	DC9	0.034	Y	330	261.6	-50.5	28	40
11/Oct	757	0.039	Y	390	196.5	-54.8	5	10
16/Oct	DC9	0.034	Y	330	261.6	-51	22	40
16/Oct	757	0.039	Y	370	216.3	-51.2	1	10
16/Oct	MD80	0.034	N	330	261.6	-51	22	40
16/Oct	727	0.034	N	330	261.6	-51	22	40

Date	Aircraft Type	Contrail Factor (g/kg-°C)	Contrail	Flight Level (kft)	Pressure (mb)	Ambient Temp (°C)	RH (In Situ)	RH (40/70/10)
16/Oct	737	0.039*	Y	330	261.6	-51	22	40
16/Oct	DC9	0.034	Y	350	238	-52.3	12	70
17/Oct	757	0.039	Y	370	216.3	-53.6	4	40
17/Oct	767	0.039	Y	350	238	-51.1	14	40
17/Oct	757	0.039	Y	370	216.3	-53.6	4	40
17/Oct	757	0.039	Y	370	216.3	-53.6	4	40
17/Oct	757	0.039	Y	390	196.5	-56.4	2	40
17/Oct	757	0.039	Y	370	216.3	-53.6	4	40
17/Oct	AIRBUS320	0.039	Y	350	238	-51.1	14	40
17/Oct	DC9	0.034	N	330	261.6	-48.3	17	40
17/Oct	737	0.039*	N	330	261.6	-48.3	17	40

Note: Aircraft whose contrail factors are marked by an asterisk are assumed to be high

bypass.

Appendix D: Propulsion Efficiency Calculations

This appendix shows the MATHCAD calculations needed to determine the propulsion efficiencies for typical low and high bypass engines.

Variables:

SFC = specific fuel consumption
mF = fuel flow rate per engine
F = thrust per engine
V = cruise speed
h = propulsion efficiency
Q = specific combustion heat

Constant:

$Q := 43 \cdot M \cdot J \cdot kg^{-1}$ (Schumann, 1996b:12)

Low Bypass Engine Calculation:

The propulsion efficiency for a typical low bypass engine was obtained by averaging engine and airframe parameters for a number of low bypass aircraft (DC-9, MD-80, MD-88, B727, B737) observed during the WPAFB data collection.

Determination of Average Cruise Speed (Montgomery and Foster, 1992:158,160,162):

$V_{DC9} := 909 \cdot km \cdot hr^{-1}$

$V_{MD80} := 909 \cdot km \cdot hr^{-1}$

$V_{MD88} := 909 \cdot km \cdot hr^{-1}$

$V_{B727} := 917 \cdot km \cdot hr^{-1}$

$V_{B737} := 907 \cdot km \cdot hr^{-1}$

$$V_{ave} := \frac{V_{DC9} + V_{MD80} + V_{MD88} + V_{B727} + V_{B737}}{5}$$

$V_{ave} = 910.2 \cdot km \cdot hr^{-1}$

Determination of Average Thrust per Engine (Lambert and Munson, 1994:749):

Note: Values given are for the Pratt&Whitney JT8D at maximum cruise at 35,000 feet

$F_{JT8D\_9} := 18.2kN$ (DC-9)

$F_{JT8D\_11} := 17.6kN$ (DC-9)

$F_{JT8D\_15} := 18.2kN$ (B727,737)

$F_{JT8D\_17} := 18.9kN$ (B727,737)

$$F_{ave} := \frac{F_{JT8D\_9} + F_{JT8D\_11} + F_{JT8D\_15} + F_{JT8D\_17}}{4}$$

$F_{ave} = 18.225kN$

Determination of Average Specific Fuel Consumption (Lambert and Munson, 1994:749):

Note: Values given are for the Pratt&Whitney JT8D at maximum cruise at 35,000 feet

$SFC_{JT8D\_9} := 22.86mg \cdot N^{-1} \cdot s^{-1}$ (DC-9)

$SFC_{JT8D\_11} := 23.14mg \cdot N^{-1} \cdot s^{-1}$ (DC-9)

$SFC_{JT8D\_15} := 22.97mg \cdot N^{-1} \cdot s^{-1}$ (B727,737)

$SFC_{JT8D\_17} := 23.37mg \cdot N^{-1} \cdot s^{-1}$ (B727,737)

$$SFC_{ave} := \frac{SFC_{JT8D\_9} + SFC_{JT8D\_11} + SFC_{JT8D\_15} + SFC_{JT8D\_17}}{4}$$

$SFC_{ave} = 23.085 \cdot mg \cdot N^{-1} \cdot s^{-1}$

Determination of Average Fuel Flow Rate per Engine (Schumann, 1996b:12):

$m_{F\_ave} := F_{ave} \cdot SFC_{ave}$

$m_{F\_ave} = 0.420724 kg \cdot sec^{-1}$

Determination of Average Propulsion Efficiency (Schumann, 1996b:12):

$$\eta_{ave} := \frac{F_{ave} \cdot V_{ave}}{m_{F\_ave} \cdot Q}$$

$\eta_{ave} = 0.254704$

This value of h is typical for low bypass aircraft observed in sector 98 airspace at cruise speed.

High Bypass Engine Calculation:

The propulsion efficiency for a modern wide body aircraft (equipped with high bypass engines) was obtained from parameters given in the Schumann paper (Schumann, 1996b:12):

$$V := 247 \cdot m \cdot s^{-1}$$

$$F := 31.1 \cdot kN$$

$$SFC := 18.7 \cdot mg \cdot N^{-1} \cdot s^{-1}$$

$$m_F := F \cdot SFC$$

$$m_F = 0.58157 \, kg \cdot sec^{-1}$$

$$\eta := \frac{F \cdot V}{m_F \cdot Q}$$

$$\eta = 0.307176$$

Appendix E: Calculation of Statistics

This appendix contains the MATHCAD program used to calculate the statistics for the Schumann, Hanson, and Schrader (AFGWC) contrail forecast algorithms using the WPAFB "dry" atmosphere data.

$ORIGIN \equiv 1$

Definition of Units:

$s := sec \qquad J := kg \cdot m^2 \cdot s^{-2} \qquad mb := 10^2 \cdot Pa \qquad M := 10^6$

Definition of Constants:

$c_p := 1004 \cdot J \cdot K^{-1} \cdot kg^{-1} \qquad \varepsilon := 0.622$

Set Relative Humidity Values (9=In Situ, 10=Assumed):

$m := 9$

Read in Table of Data to be Analyzed:

$Data := READPRN(wpdry) \qquad$ (Disk #2)

Column 1: Date of Observation   Column 6: Flight Level (kft)
Column 2: Aircraft Type   Column 7: Pressure at Flight Level (mb)
Column 3: Contrail Factor   Column 8: Ambient Temperature (C)
Column 4: Propulsion Efficiency   Column 9: RH (In Situ)
Column 5: Contrail? (1=yes, 0=no)   Column 10: RH (Assumed)

Definition of Variables:

$p := Data^{\langle 7 \rangle} \qquad$ (Flight Level Pressure)

$T_E := Data^{\langle 8 \rangle} \qquad$ (Ambient Temperature) $\quad T_E := T_E \cdot K$

$Con := Data^{\langle 5 \rangle} \qquad$ (Contrail Observation)

$U := Data^{\langle m \rangle} \qquad$ (Relative Humidity) $\quad U := \dfrac{U}{100}$

$CF := Data^{\langle 3 \rangle} \qquad$ (Contrail Factor)

$\eta := Data^{\langle 4 \rangle} \qquad$ (Propulsion Efficiency)

Definition of Goff-Gratch Formula for Saturation Vapor Pressure with Respect to Water:

$$GG1 := 23.832241 \qquad\qquad GG5 := 8.1328 \cdot 10^{-3}$$

$$GG2(T) := 5.02808 \cdot \log(T)$$

$$GG6(T) := 10^{\left(3.49149 - \frac{1302.8844}{T}\right)}$$

$$GG3 := 1.3816 \cdot 10^{-7}$$

$$GG4(T) := 10^{(11.334 - 0.0303998 \cdot T)} \qquad GG7(T) := \frac{2949.076}{T}$$

$$e_s(T) := 10^{GG1 - GG2(T) - GG3 \cdot GG4(T) + GG5 \cdot GG6(T) - GG7(T)} \cdot mb$$

(Enter temperature in Kelvin)

1. Schumann Forecast Method Calculations:

Calculation of the (Variable) "Contrail Factor" or Slope of the Mixing Line (Schumann, 1996b:9):

$$i := 1 .. \text{rows}(Data) \qquad EI_{H2O} := 1.25 \cdot kg \cdot kg^{-1} \qquad Q := 43 \cdot M \cdot J \cdot kg^{-1} \qquad p := p \cdot mb$$

$$G_i := \frac{EI_{H2O} \cdot c_p \cdot p_i}{\varepsilon \cdot Q \cdot \left(1 - \eta_i\right)} \qquad G := G \cdot K \cdot Pa^{-1} \quad \text{(convert to unitless value for empirical equation)}$$

Calculation of the Temperature at which the Mixing Line Just Touches the Saturation
 Vapor Pressure Curve under Threshold Conditions where Ambient Temperature
=Critical Temperature (Schumann, 1996b:18):

$$T_{LM_i} := -46.46 + 9.43 \cdot \ln\left(G_i - 0.053\right) + 0.720 \cdot \left(\ln\left(G_i - 0.053\right)\right)^2$$

(empirical formula: T_{LM} in deg C, G in PaK^{-1})

$$T_{LM} := T_{LM} \cdot K + 273.15 \cdot K \qquad \text{(convert } T_{LM} \text{ to Kelvin)}$$

$$T_{LM} := T_{LM} \cdot K^{-1} \qquad \text{(convert } T_{LM} \text{ to unitless value)}$$

$$G := G \cdot K^{-1} \cdot Pa \qquad \text{(convert G from unitless value)}$$

Evaluate Derivatives of the Goff-Gratch Equation at T_{LM}:

$$D1\left(T_{LM}\right) := \frac{d}{dT_{LM}} e_s\left(T_{LM}\right) \qquad \text{(first derivative)}$$

$$D2\left(T_{LM}\right) := \frac{d^2}{dT_{LM}^2} e_s\left(T_{LM}\right) \qquad \text{(second derivative)}$$

Calculation the Critical Temperature for Contrail Formation by a Taylor Series Expansion about T_{LM} (Schumann, 1996b:18):

$$A\left(T_{LM}\right) := \frac{\left(1 - U_i\right) \cdot G_i}{\left(U_i\right)^2 \cdot D2\left(T_{LM_i}\right)} \cdot K^2$$

$$e_E\left(T_{LM}\right) := U_i \cdot e_s\left(T_{LM_i}\right)$$

$$B\left(T_{LM}\right) := \frac{e_s\left(T_{LM_i}\right) - e_s\left(T_{LM_i}\right) \cdot U_i}{\left(U_i\right)^2 \cdot D2\left(T_{LM_i}\right)} \cdot K^2$$

$$x_i := -A\left(T_{LM}\right) + \sqrt{\left(A\left(T_{LM}\right)\right)^2 + 2 \cdot B\left(T_{LM}\right)}$$

$$T_{LC_i} := T_{LM_i} \cdot K - x_i \qquad \text{(critical temperature for contrail formation)}$$

$$T_{LC_i} := T_{LC_i} - 273.15 \cdot K \qquad \text{(convert to degrees Celsius)}$$

Compare Critical Temperatures to Ambient Temperatures and Contrail Observations:

$$\text{Diff}_{S_i} := T_{LC_i} - T_{E_i} \qquad \text{(difference between critical temperature and ambient temperature at each flight level)}$$

$$\text{Diff}_S := \text{Diff}_S \cdot K^{-1}$$

87

If the difference between the critical temperature and ambient temperature is greater than zero (the environment is colder than the critical temperature), forecast contrails at that altitude.

2. Hanson Forecast Method Calculations:

<u>Definition of Goff-Gratch Formula for Saturation Vapor Pressure with Respect to Water</u>:

$$e_w(T) := 10^{GG1 - GG2(T) - GG3 \cdot GG4(T) + GG5 \cdot GG6(T) - GG7(T)}$$

<u>Definition of Terms Resulting from the Differentiation of the Goff-Gratch Equation with Respect to Temperature</u> (Hanson and Hanson, 1995:2401):

$$P1(T) := 23.83224 + 8.132801 \cdot 10^{-3} \cdot \left[10^{\left(3.49149 - \frac{1302.8844}{T}\right)} \right]$$

$$P2(T) := 1.3816 \cdot 10^{-7} \cdot 10^{(11.334 - 0.0303998 \cdot T)}$$

$$P3(T) := \frac{2949.076}{T}$$

$$P4(T) := 5.02808 \cdot \frac{\ln(T)}{\ln(10)}$$

$$P5(T) := \frac{2949.08}{T^2}$$

$$P6(T) := \frac{5.02808}{T \cdot \ln(10)}$$

$$P7(T) := 4.20004 \cdot 10^{-9} \cdot \left[10^{(11.334 - 0.0303998 \cdot T)} \right] \cdot \ln(10)$$

$$P8(T) := 10.5961 \cdot \frac{10^{\left(3.49149 - \frac{1302.8844}{T}\right)}}{T^2} \cdot \ln(10)$$

Redefinition of Variables used in the Hanson Equations:

ORIGIN ≡ 1

$i := 1 .. \text{rows}(\text{Data})$

$p := \text{Data}^{<7>}$ (Flight Level Pressure)

$T_E := \text{Data}^{<8>}$ (Ambient Temperature) $T_E := T_E \cdot K$

$\text{Con} := \text{Data}^{<5>}$ (Contrail Observation)

$\text{RH} := \text{Data}^{<m>}$ (Relative Humidity)

$\text{CF} := \text{Data}^{<3>}$ (Contrail Factor)

Calculation of the Critical Temperature for Contrail Formation by Using the Secant Method to Find the Root of the Following Relationship
(Hanson and Hanson, 1995:2403):

$T := 240$ (first guess at temperature)

$$f(T) := \left(\frac{100}{\text{RH}_i}\right) \cdot \left[10^{(P1(T) - P2(T) - P3(T) - P4(T))} \cdot \ln(10) \cdot (P5(T) - P6(T) + P7(T) + P8(T)) \right] - \frac{p_i \cdot CF_i}{622}$$

$T_{C_i} := \text{root}(f(T), T)$ (find root using first guess)

$T_C := T_C - 273.15$ (convert to degrees Celsius)

$T_C := T_C \cdot K$

Compare Critical Temperatures to Ambient Temperatures and Contrail Observations:

$\text{Diff}_H := T_C - T_E$ (difference between critical temperature and ambient temperature at each flight level)

If the difference between the critical temperature and ambient temperature is greater than zero (the environment is colder than the critical temperature), forecast contrails at that altitude.

3. Schrader (AFGWC) Forecast Method Calculations:

Definition of Goff-Gratch Formula for Saturation Vapor Pressure with Respect to Water:

$$e_s(T_d) := 10^{\left[23.832241 - 5.02808 \cdot \log(T_d) - 1.3816 \cdot 10^{-7} \cdot 10^{\left(11.334 - 0.0303998 \cdot T_d\right)} \; \cdots \; + 8.1328 \cdot 10^{-3} \cdot 10^{\left(3.49149 - \frac{1302.8844}{T_d}\right)} \right] - \frac{2949.076}{T_d}}$$

Term used in the Derivative of the Goff-Gratch Formula with Respect to Temperature:

$$D(T_d) := \left[\left[\left[\frac{-5.02808}{\left(T_d \cdot \ln(10)\right)} \; \cdots \; + 4.200036368 \cdot 10^{-9} \cdot 10^{\left(11.334 - 3.03998 \cdot 10^{-2} \cdot T_d\right)} \cdot \ln(10) \right] \; \cdots \; + 10.59609824832 \cdot \frac{10^{\left(3.49149 - \frac{1302.8844}{T_d}\right)}}{T_d^2} \cdot \ln(10) \right] + \frac{2949.076}{T_d^2} \right] \cdot \ln(10)$$

Derivative of the Goff-Gratch Formula with Respect to Temperature:

$$dere_s(T_d) := 10^{\left[\left[23.832241 - 5.02808 \cdot \frac{\ln(T_d)}{\ln(10)} - 1.3816 \cdot 10^{-7} \cdot 10^{\left(11.334 - 3.03998 \cdot 10^{-2} \cdot T_d\right)} \; \cdots \; + 8.1328 \cdot 10^{-3} \cdot 10^{\left(3.49149 - \frac{1302.8844}{T_d}\right)} \right] - \frac{2949.076}{T_d} \right]} \cdot D(T_d)$$

Relationship at the Critical Temperature for Contrail Formation where the Slope of the Mixing Line Equals the Slope of the Goff-Gratch Equation (Schrader, 1994:7-8):

$$C_F \cdot \frac{p}{622} = dere_s(T_d)$$

Calculation of the Critical Temperature for Contrail Formation at 100 Percent Relative Humidity by Using the Secant Method to Find the Root of the Following Equation (Schrader, 1994:8):

$T_d := 250$ (first guess at critical temperature) $i := 1 .. \text{rows(Data)}$

$$f\left(T_d\right) := \text{dere}_s\left(T_d\right) - CF_i \cdot \frac{P_i}{622}$$

$T_{Crit\_100_i} := \text{root}\left(f\left(T_d\right), T_d\right)$ (find root using first guess)

$T_{Crit\_100} := T_{Crit\_100} - 273.15$ (convert to degrees Celsius)

$T_{Crit\_100_i} := T_{Crit\_100_i} + 273.15$ (convert back to K to calculate critical temperatures at variable relative humidity values)

Calculation of the Critical Temperature for Contrail Formation at Variable Relative Humidity by Using the Secant Method to Find the Root of the Following Equation (Schrader, 1994:8-9):

$T_{Crit\_RH} := 170$ (first guess at critical temperature)

$$f\left(T_{Crit\_RH}\right) := \frac{e_s\left(T_{Crit\_100_i}\right) - \left(T_{Crit\_100_i} - T_{Crit\_RH}\right) \cdot \text{dere}_s\left(T_{Crit\_100_i}\right)}{e_s\left(T_{Crit\_RH}\right)} \cdot 100 - RH_i$$

$T_{Crit\_RH_i} := \text{root}\left(f\left(T_{Crit\_RH}\right), T_{Crit\_RH}\right)$ (find root using first guess)

$T_{Crit\_RH} := T_{Crit\_RH} - 273.15$ (convert to degrees Celsius)

$T_{Crit\_RH} := T_{Crit\_RH} \cdot K$

Compare Critical Temperatures to Ambient Temperatures and Contrail Observations:

$$\text{Diff}_{\text{AFWC}} := T_{\text{Crit\_RH}} - T_E$$

(difference between critical temperature and ambient temperature at each flight level)

If the difference between the critical temperature and ambient temperature is greater than zero (the environment is colder than the critical temperature), forecast contrails at that altitude.

4. Calculation of Statistics Using the Schumann Forecast Method:

$$n := \text{rows}(\text{Data}) \quad \text{(sample size)}$$

Determine the Number of Times Contrails Were Forecast and Were Observed:

$$a\left(\text{Diff}_S, \text{Con}, n\right) := \sum_{i=1}^{n} \text{if}\left[\left[\left(\text{Diff}_{S_i} > 0\right) + \left(\text{Con}_i = 1\right)\right] = 2, 1, 0\right] \qquad a\left(\text{Diff}_S, \text{Con}, n\right) = 33$$

Determine the Number of Times Contrails Were Forecast and Were Not Observed:

$$b\left(\text{Diff}_S, \text{Con}, n\right) := \sum_{i=1}^{n} \text{if}\left[\left[\left(\text{Diff}_{S_i} > 0\right) + \left(\text{Con}_i = 0\right)\right] = 2, 1, 0\right] \qquad b\left(\text{Diff}_S, \text{Con}, n\right) = 5$$

Determine the Number of Times Contrails Were Not Forecast and Were Observed:

$$c\left(\text{Diff}_S, \text{Con}, n\right) := \sum_{i=1}^{n} \text{if}\left[\left[\left(\text{Diff}_{S_i} < 0\right) + \left(\text{Con}_i = 1\right)\right] = 2, 1, 0\right] \qquad c\left(\text{Diff}_S, \text{Con}, n\right) = 11$$

Determine the Number of Times Contrails Were Not Forecast and Were Not Observed:

$$d\left(\text{Diff}_S, \text{Con}, n\right) := \sum_{i=1}^{n} \text{if}\left[\left[\left(\text{Diff}_{S_i} < 0\right) + \left(\text{Con}_i = 0\right)\right] = 2, 1, 0\right] \qquad d\left(\text{Diff}_S, \text{Con}, n\right) = 16$$

<u>Define 2 X 2 Contingency Table Entries</u>:

$A_S := a(\text{Diff}_S, \text{Con}, n)$ $A_S = 33$

$B_S := b(\text{Diff}_S, \text{Con}, n)$ $B_S = 5$

$C_S := c(\text{Diff}_S, \text{Con}, n)$ $C_S = 11$

$D_S := d(\text{Diff}_S, \text{Con}, n)$ $D_S = 16$

$$\text{Ctable}_S := \begin{pmatrix} A_S & B_S \\ C_S & D_S \end{pmatrix} \qquad \text{Ctable}_S = \begin{pmatrix} 33 & 5 \\ 11 & 16 \end{pmatrix}$$

Element 1,1: Contrail Fcst, Observed
Element 1,2: Contrail Fcst, Not Observed
Element 2,1: Contrail Not Fcst, Observed
Element 2,2: Contrail Not Fcst, Not Observed

$n := A_S + B_S + C_S + D_S$ $n = 65$ (sample size)

A. Statistical Measures of Accuracy:

<u>Hit Rate (H)</u>: $H_{\text{Schumann}} := \dfrac{A_S + D_S}{n}$ $H_{\text{Schumann}} = 0.754$

<u>Percent Correct (PFC)</u>: $PFC_{\text{Schumann}} := H_{\text{Schumann}} \cdot 100$ $PFC_{\text{Schumann}} = 75.385$

<u>Critical Success Index (CSI)</u>: $CSI_{\text{Schumann}} := \dfrac{A_S}{A_S + B_S + C_S}$ $CSI_{\text{Schumann}} = 0.673$

<u>False Alarm Rate (FAR)</u>: $FAR_{\text{Schumann}} := \dfrac{B_S}{A_S + B_S}$ $FAR_{\text{Schumann}} = 0.132$

B. Indicator of Bias:

<u>Bias Ratio (B)</u>: $\text{Bias}_{\text{Schumann}} := \dfrac{A_S + B_S}{A_S + C_S}$ $\text{Bias}_{\text{Schumann}} = 0.864$

B<1: event forecast less often than observed *(underforecast)*
B>1: event forecast more often than observed *(overforecast)*

C. Skill Measures:

Hanssen-Kuipers Discriminant (HKD): $\text{HKD}_{\text{Schumann}} := \dfrac{\left(A_S \cdot D_S\right) - \left(B_S \cdot C_S\right)}{\left(A_S + C_S\right) \cdot \left(B_S + D_S\right)}$

$$\text{HKD}_{\text{Schumann}} = 0.512$$

5. Calculation of Statistics Using the Hanson Forecast Method:

$\quad$ n := rows(Data)   (sample size)

Determine the Number of Times Contrails Were Forecast and Were Observed:

$$a\left(\text{Diff}_H, \text{Con}, n\right) := \sum_{i=1}^{n} \text{if}\left[\left[\left(\text{Diff}_{H_i} > 0\right) + \left(\text{Con}_i = 1\right)\right] = 2, 1, 0\right] \qquad a\left(\text{Diff}_H, \text{Con}, n\right) = 0$$

Determine the Number of Times Contrails Were Forecast and Were Not Observed:

$$b\left(\text{Diff}_H, \text{Con}, n\right) := \sum_{i=1}^{n} \text{if}\left[\left[\left(\text{Diff}_{H_i} > 0\right) + \left(\text{Con}_i = 0\right)\right] = 2, 1, 0\right] \qquad b\left(\text{Diff}_H, \text{Con}, n\right) = 0$$

Determine the Number of Times Contrails Were Not Forecast and Were Observed:

$$c\left(\text{Diff}_H, \text{Con}, n\right) := \sum_{i=1}^{n} \text{if}\left[\left[\left(\text{Diff}_{H_i} < 0\right) + \left(\text{Con}_i = 1\right)\right] = 2, 1, 0\right] \qquad c\left(\text{Diff}_H, \text{Con}, n\right) = 44$$

Determine the Number of Times Contrails Were Not Forecast and Were Not Observed:

$$d\left(\text{Diff}_H, \text{Con}, n\right) := \sum_{i=1}^{n} \text{if}\left[\left[\left(\text{Diff}_{H_i} < 0\right) + \left(\text{Con}_i = 0\right)\right] = 2, 1, 0\right] \qquad d\left(\text{Diff}_H, \text{Con}, n\right) = 21$$

<u>Define 2 X 2 Contingency Table Entries:</u>

$$A_H := a\left(\text{Diff}_H, \text{Con}, n\right) \qquad A_H = 0$$

$$B_H := b\left(\text{Diff}_H, \text{Con}, n\right) \qquad B_H = 0$$

$$C_H := c\left(\text{Diff}_H, \text{Con}, n\right) \qquad C_H = 44$$

$$D_H := d\left(\text{Diff}_H, \text{Con}, n\right) \qquad D_H = 21$$

$$\text{Ctable}_H := \begin{pmatrix} A_H & B_H \\ C_H & D_H \end{pmatrix} \qquad \text{Ctable}_H = \begin{pmatrix} 0 & 0 \\ 44 & 21 \end{pmatrix}$$

Element 1,1: Contrail Fcst, Observed
Element 1,2: Contrail Fcst, Not Observed
Element 2,1: Contrail Not Fcst, Observed
Element 2,2: Contrail Not Fcst, Not Observed

$$n := A_H + B_H + C_H + D_H \qquad n = 65 \qquad \text{(sample size)}$$

A. Statistical Measures of Accuracy:

<u>Hit Rate (H):</u>
$$H_{Hanson} := \frac{A_H + D_H}{n} \qquad\qquad H_{Hanson} = 0.323$$

<u>Percent Correct (PFC):</u>
$$PFC_{Hanson} := H_{Hanson} \cdot 100 \qquad PFC_{Hanson} = 32.308$$

<u>Critical Success Index (CSI):</u>
$$CSI_{Hanson} := \frac{A_H}{A_H + B_H + C_H} \qquad CSI_{Hanson} = 0$$

<u>False Alarm Rate (FAR):</u>
$$FAR_{Hanson} := \frac{B_H}{A_H + B_H} \qquad FAR_{Hanson} = 0$$

B. Indicator of Bias:

<u>Bias Ratio (B):</u>
$$\text{Bias}_{Hanson} := \frac{A_H + B_H}{A_H + C_H} \qquad \text{Bias}_{Hanson} = 0$$

C. Skill Measures:

<u>Hanssen-Kuipers Discriminant (HKD):</u> $HKD_{Hanson} := \dfrac{\left(A_H \cdot D_H\right) - \left(B_H \cdot C_H\right)}{\left(A_H + C_H\right) \cdot \left(B_H + D_H\right)}$

$$HKD_{Hanson} = 0$$

6. Calculation of Statistics Using the Schrader (AFGWC) Forecast Method:

$n := rows(Data)$ (sample size)

<u>Determine the Number of Times Contrails Were Forecast and Were Observed:</u>

$$a\left(Diff_{AFWC}, Con, n\right) := \sum_{i=1}^{n} if\left[\left[\left(Diff_{AFWC_i} > 0\right) + \left(Con_i = 1\right)\right] = 2, 1, 0\right] \quad a\left(Diff_{AFWC}, Con, n\right) = 32$$

<u>Determine the Number of Times Contrails Were Forecast and Were Not Observed:</u>

$$b\left(Diff_{AFWC}, Con, n\right) := \sum_{i=1}^{n} if\left[\left[\left(Diff_{AFWC_i} > 0\right) + \left(Con_i = 0\right)\right] = 2, 1, 0\right] \quad b\left(Diff_{AFWC}, Con, n\right) = 5$$

<u>Determine the Number of Times Contrails Were Not Forecast and Were Observed:</u>

$$c\left(Diff_{AFWC}, Con, n\right) := \sum_{i=1}^{n} if\left[\left[\left(Diff_{AFWC_i} < 0\right) + \left(Con_i = 1\right)\right] = 2, 1, 0\right] \quad c\left(Diff_{AFWC}, Con, n\right) = 12$$

<u>Determine the Number of Times Contrails Were Not Forecast and Were Not Observed:</u>

$$d\left(Diff_{AFWC}, Con, n\right) := \sum_{i=1}^{n} if\left[\left[\left(Diff_{AFWC_i} < 0\right) + \left(Con_i = 0\right)\right] = 2, 1, 0\right] \quad d\left(Diff_{AFWC}, Con, n\right) = 16$$

Define 2 X 2 Contingency Table Entries:

$$A_{AFWC} := a\left(Diff_{AFWC}, Con, n\right) \qquad\qquad A_{AFWC} = 32$$

$$B_{AFWC} := b\left(Diff_{AFWC}, Con, n\right) \qquad\qquad B_{AFWC} = 5$$

$$C_{AFWC} := c\left(Diff_{AFWC}, Con, n\right) \qquad\qquad C_{AFWC} = 12$$

$$D_{AFWC} := d\left(Diff_{AFWC}, Con, n\right) \qquad\qquad D_{AFWC} = 16$$

$$Ctable_{AFWC} := \begin{pmatrix} A_{AFWC} & B_{AFWC} \\ C_{AFWC} & D_{AFWC} \end{pmatrix}$$

Element 1,1: Contrail Fcst, Observed
Element 1,2: Contrail Fcst, Not Observed
Element 2,1: Contrail Not Fcst, Observed
Element 2,2: Contrail Not Fcst, Not Observed

$$Ctable_{AFWC} = \begin{pmatrix} 32 & 5 \\ 12 & 16 \end{pmatrix}$$

$$n := A_{AFWC} + B_{AFWC} + C_{AFWC} + D_{AFWC} \qquad n = 65 \qquad \text{(sample size)}$$

A. Statistical Measures of Accuracy:

Hit Rate (H): $H_{AFWC} := \dfrac{A_{AFWC} + D_{AFWC}}{n}$ $\qquad\qquad H_{AFWC} = 0.738$

Percent Correct (PFC): $PFC_{AFWC} := H_{AFWC} \cdot 100$ $\qquad PFC_{AFWC} = 73.846$

Critical Success Index (CSI): $CSI_{AFWC} := \dfrac{A_{AFWC}}{A_{AFWC} + B_{AFWC} + C_{AFWC}}$ $\qquad CSI_{AFWC} = 0.653$

False Alarm Rate (FAR): $FAR_{AFWC} := \dfrac{B_{AFWC}}{A_{AFWC} + B_{AFWC}}$ $\qquad FAR_{AFWC} = 0.135$

B. Indicator of Bias:

$\underline{\text{Bias Ratio}}$ (B): $\text{Bias}_{\text{AFWC}} := \dfrac{A_{\text{AFWC}} + B_{\text{AFWC}}}{A_{\text{AFWC}} + C_{\text{AFWC}}}$ $\text{Bias}_{\text{AFWC}} = 0.841$

C. Skill Measures:

$\underline{\text{Hanssen-Kuipers Discriminant}}$ (HKD):

$$\text{HKD}_{\text{AFWC}} := \dfrac{\left(A_{\text{AFWC}} \cdot D_{\text{AFWC}} \right) - \left(B_{\text{AFWC}} \cdot C_{\text{AFWC}} \right)}{\left(A_{\text{AFWC}} + C_{\text{AFWC}} \right) \cdot \left(B_{\text{AFWC}} + D_{\text{AFWC}} \right)}$$

$$\text{HKD}_{\text{AFWC}} = 0.489$$

7. Statistical Summary:

$H_{\text{Schumann}} = 0.754$ $H_{\text{Hanson}} = 0.323$ $H_{\text{AFWC}} = 0.738$

$\text{PFC}_{\text{Schumann}} = 75.385$ $\text{PFC}_{\text{Hanson}} = 32.308$ $\text{PFC}_{\text{AFWC}} = 73.846$

$\text{CSI}_{\text{Schumann}} = 0.673$ $\text{CSI}_{\text{Hanson}} = 0$ $\text{CSI}_{\text{AFWC}} = 0.653$

$\text{FAR}_{\text{Schumann}} = 0.132$ $\text{FAR}_{\text{Hanson}} = 0$ $\text{FAR}_{\text{AFWC}} = 0.135$

$\text{Bias}_{\text{Schumann}} = 0.864$ $\text{Bias}_{\text{Hanson}} = 0$ $\text{Bias}_{\text{AFWC}} = 0.841$

$\text{HKD}_{\text{Schumann}} = 0.512$ $\text{HKD}_{\text{Hanson}} = 0$ $\text{HKD}_{\text{AFWC}} = 0.489$

Bibliography

Appleman, Herbert S. "The Formation of Exhaust Condensation Trails by Jet Aircraft," Bull. Amer. Meteor. Soc., 34: 14-20 (January 1953).

-----. Derivation of Jet-Aircraft Contrail-Formation Curves. AWS TR 105-145. Washington: HQ AWS, January 1957.

Bjornson, Brian M. SAC Contrail Formation Study. USAFETAC/PR-92/003. Scott AFB, Illinois: HQ USAFETAC, May 1992.

Brock, Fred V. and Carol E. Nicolaidis. Instructor's Handbook on Meteorological Instrumentation. Boulder, CO: National Center for Atmospheric Research, July 1985 (NCAR/TN-237+1A).

Coleman, Rich F. "A New Formulation for the Critical Temperature for Contrail Formation," J. Appl. Meteor., 35: 2270-2282 (December 1996).

Department of the Air Force. Forecasting Aircraft Condensation Trails. AWS/TR-81/001. Scott AFB, Illinois: HQ AWS, September 1981.

Devore, Jay L. Probability and Statistics for Engineering and the Sciences. Belmont, CA: Wadsworth Publishing Company, 1995.

Federal Aviation Administration. Federal Aviation Regulation Part 91. Washington: November 1990.

Hanson, Harvey M. and Douglas M. Hanson. "A Reexamination of the Formation of Exhaust Condensation Trails by Jet Aircraft," J. Appl. Meteor., 34: 2400-2405 (December 1995).

Kalbfleisch, J.G. Probability and Statistical Inference II. New York: Springer-Verlag, 1979.

Lambert, Mark and Kenneth Munson. Jane's All the World's Aircraft 1994-1995. London: Butler and Tanner Ltd, 1994.

Montgomery, M. R. and Gerald R. Foster. A Field Guide to Airplanes of North America. Boston: Houghton Mifflin Company, 1992.

Peters, Jeffrey L. New Techniques for Contrail Forecasting. AWS/TR-93/001. Scott AFB, Illinois: HQ AWS, August 1993.

Polander, John. Staff Meteorological Officer, United States Air Force, Wright-Patterson AFB OH. Personal communication. November 1996.

Reynolds, Daniel E. Assistant Professor of Statistics, Air Force Institute of Technology, Wright-Patterson AFB OH. Personal communication. March 1997.

Rogers, Roddy R. and M.K. Yau. A Short Course in Cloud Physics. New York: Pergamon, 1994.

Saatzer, P. Pilot Alert System Flight Test: Final Technical Report, November 1988-May 1993. Pico Rivera CA: B-2 Division Northrop Grumman Corporation, February 1995.

Sachs, Lothar. Applied Statistics: A Handbook of Techniques. New York: Springer-Verlag, 1984.

Schrader, Mark L. "Calculations of Critical Temperature of Contrail Formation for Different Engine Types." Unpublished Report. HQ AWS, Scott AFB IL, 1994.

Schumann, Ulrich "Comments on A Reexamination of the Formation of Exhaust Condensation Trails by Jet Aircraft," J. Appl. Meteor., 35: 2283-2284 (December 1996).

-----. "On Conditions for Contrail Formation from Aircraft Exhausts," Meteorologisch Zeitschrift, N.F. 5: 4-23 (February 1996).

Wallace, John M. and Peter V. Hobbs. Atmospheric Science An Introductory Survey. New York: Academic Press, 1977.

Wilks, Daniel S. Statistical Methods in the Atmospheric Sciences. New York: Academic Press, 1995.

Vita

Capt Robert P. Asbury III ████████████████████████████████. He
graduated from Radford High School in 1982 and entered undergraduate studies at
Virginia Polytechnic Institute and State University in Blacksburg, Virginia. In 1985, he
enlisted in the Air Force as an Airborne Cryptologic Linguist (Korean). He was assigned
to the 6990th Electronic Security Group at Kadena AB, Japan and flew strategic and
tactical reconnaissance missions aboard RC-135W, EC-130H, and E-3B aircraft.

After separating from the Air Force, he attended the University of Hawaii at
Manoa and graduated in July 1991 with a Bachelor of Science degree in Meteorology. He
was commissioned through the Air Force Reserve Officer Training Corps upon
graduation.

His first assignment as an officer was with the 24th Infantry Division
(Mechanized) at Fort Stewart, Georgia as a Combat Weather Team Officer in Charge. In
August 1995, he entered the school of Engineering Physics, Air Force Institute of
Technology. Upon graduation, Captain Asbury will be assigned to Phillips Laboratory at
Kirtland AFB, New Mexico as a Staff Meteorologist.

Captain Asbury is married to the former Eileen Cearley of Deer Lodge, Montana.
They have two daughters, Jessica and Julie.

████████████████████████

1. AGENCY USE ONLY (Leave blank)	2. REPORT DATE March 1997	3. REPORT TYPE AND DATES COVERED Master's Thesis

4. TITLE AND SUBTITLE

AN EXAMINATION OF THE HANSON CONTRAIL FORECAST ALGORITHM UNDER LOW RELATIVE HUMIDITY CONDITIONS

5. FUNDING NUMBERS

6. AUTHOR(S)

Robert P. Asbury III, Captain, USAF

7. PERFORMING ORGANIZATION NAME(S) AND ADDRESS(ES)

Air Force Institute of Technology
2750 P Street
WPAFB OH 45433-7765

8. PERFORMING ORGANIZATION REPORT NUMBER

AFIT/GM/ENP/97M-01

9. SPONSORING/MONITORING AGENCY NAME(S) AND ADDRESS(ES)

88th Weather Squadron
Mr. Steve Weaver
2049 Monhan Way, Bldg 91, Area B
WPAFB OH 45433-2704

10. SPONSORING/MONITORING AGENCY REPORT NUMBER

11. SUPPLEMENTARY NOTES

12a. DISTRIBUTION/AVAILABILITY STATEMENT

Approved for public release; distribution unlimited

12b. DISTRIBUTION CODE

13. ABSTRACT (Maximum 200 words)

Accurate forecasts of contrail occurrence are essential to military aircrews. Although classical forecast methods have been reasonably successful predicting contrails, there is need for improvement at low ambient relative humidity. This thesis examines the performance of the Hanson method, which was developed to provide better contrail forecasts under drier atmospheric conditions. As a secondary objective, the forecast methods of Schumann and Hanson are compared to the algorithm currently in use by the Air Force Global Weather Central. Data used to validate the algorithms were collected at Wright-Patterson AFB, OH and Edwards AFB, CA. Theoretical contrail forecasts were made for each observation, using the flight level pressure, ambient temperature, and relative humidity. Comparisons were then made between the forecast and actual observation of contrail conditions. Forecast and occurrence data were then statistically analyzed to gauge each method's performance. All methods detected roughly 75 percent of observed contrails under moist atmospheric conditions. However, the Hanson method's performance decreased when drier atmospheric observations were tested. Schumann's method performed as well as the AFGWC algorithm under all atmospheric conditions. Based on this research, the Hanson method is not recommended for operational use.

14. SUBJECT TERMS

contrails, pressure, relative humidity, high bypass engine

15. NUMBER OF PAGES

115

16. PRICE CODE

17. SECURITY CLASSIFICATION OF REPORT	18. SECURITY CLASSIFICATION OF THIS PAGE	19. SECURITY CLASSIFICATION OF ABSTRACT	20. LIMITATION OF ABSTRACT
Unclassified	Unclassified	Unclassified	UL